Detrital zircons from late Paleozoic accretionary complexes in north-central Chile (28°–32°S): Possible fingerprints of the Chilenia terrane

J. Álvarez [a,*], C. Mpodozis [b], C. Arriagada [a], R. Astini [c], D. Morata [a], E. Salazar [a], V.A. Valencia [d], J.D. Vervoort [e]

[a] Departamento de Geología, Universidad de Chile, Plaza Ercilla 803, Santiago, Chile
[b] Antofagasta Minerals, Apoquindo 4001, Piso 18, Santiago, Chile
[c] Laboratorio de Análisis de Cuencas, CICTERRA-Universidad Nacional de Córdoba, Av. Vélez Sarsfield 1611, 2° piso, Of. 7, X5016GCA Córdoba, Argentina
[d] Valencia Geoservices, 3389 N River Rapids Dr, Tucson, AZ 85712, USA
[e] Department of Geology, Washington State University, Pullman, WA 99164-2812, USA

ARTICLE INFO

ABSTRACT

During the Paleozoic the Andean basement of central Chile and Argentina grew westwards by the amalgamation of diverse tectonostratigraphic terranes some of them derived from Laurentia. The last to be accreted, in the Devonian, corresponds to the hypothetical Chilenia terrane. However, direct evidences about the nature of its basement are scarce because volcanics and intrusives associated to a Late Paleozoic arc and the Choiyoi Large Igneous Province concealed almost all older geological units. Indirect evidences about the nature of Chilenia can be obtained from the examination of the detrital zircon age populations in late Paleozoic accretionary prisms formed after its collision along the Pacific margin of Gondwana which may have incorporated sediments derived from the erosion of the Chilenia basement. Zircon populations from three of these accretionary complexes, El Tránsito, Huasco and Choapa (north-central Chile, 28–32°S) include Ordovician (Famatinian), Cambrian (Pampean), Neoproterozoic (Brasiliano) and Mesoproterozoic (Grenvillian) zircons whose sources can be tracked to Gondwana. Nevertheless, the three complexes also include a very large subpopulation of zircons that cannot easily be traced to well-known Gondwana sources and that are derived from the erosion of late Neoproterozoic to Early Cambrian (580–530 Ma) magmatic/metamorphic sources, that possibly form a significant component of the Chilenia microcontinental basement.

1. Introduction

During most of the Paleozoic, east-directed subduction of oceanic crust of the ancestral Pacific (Iapetus) ocean, microplate collision and terrane accretion shaped the western South American segment of the Paleozoic peri-Gondwana Terra Australis Orogen (Ramos et al., 1984, 1986; Astini et al., 1995; Rapela et al., 1998; Thomas and Astini, 2003a,b; Cawood, 2005; Collo et al., 2009; Ramos, 2009). This protracted process included the collision and amalgamation to Gondwana of diverse allochthonous and/or para-autochthonous terranes like Arequipa–Antofalla, Pampia or the Cuyania composite terrane (Fig. 1). One of the latest terranes that are supposed to have been accreted during the late Devonian is the hypothetical Chilenia Terrane (Ramos et al., 1984, 1986). However,

unlike other terranes such as Pampia or Cuyania (Rapela et al., 1998; Ramos, 2009), geological evidences about the nature of the Chilenia terrane remain elusive. Inferences about its existence are largely indirect. One supporting argument in favor of the "microcontinental" nature of Chilenia can be found in the geochemical signatures of the Late Paleozoic–Triassic acid volcanic and plutonic rocks of the Choiyoi Large Igneous Province (Kay et al., 1989; Mpodozis and Kay, 1992; Llambías, 1999) These igneous rocks form much of the Frontal Cordillera of Argentina and Chile, and its petrogenesis indicates a significant contribution from melts derived from a continental basement (Mpodozis and Kay, 1992). One of the few units that have been proposed and remains as a possible candidate to be a remnant of the Chilenia sialic basement are the La Pampa Gneisses (Ribba et al., 1988). These are small outcrops of granodioritic orthogneisses that appear as enclaves within Elquí-Limarí Batholith near El Tránsito, to the east of Vallenar, in Chile (Fig. 1) from which Ribba et al. (1988) obtained a Rb–Sr of 415 ± 4 Ma age that they interpreted as an isotopic
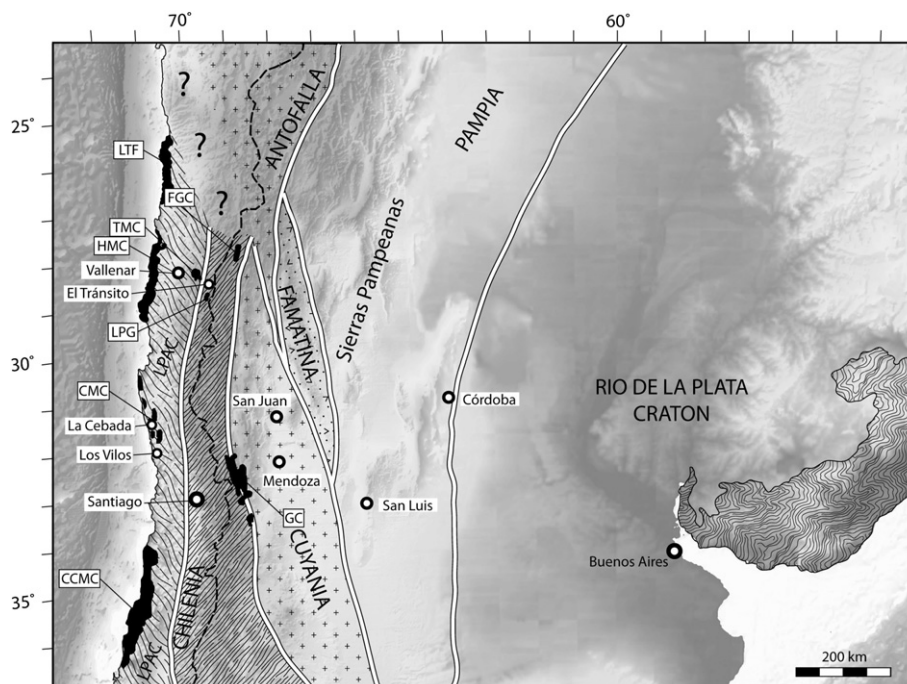
Fig. 1. Map of tectonostratigraphic terranes of Central Chile and Argentina, showing the approximate position of terrane sutures (thick white lines). In black, outcrops of the main metamorphic complexes and units discussed within the text. LPAC: Late Paleozoic Accretionary Complexes, LFT: Las Tórtolas Formation, HMC: Huasco Metamorphic Complex, LPG: La Pampa Gneisses, TMC: El Tránsito Metamorphic Complex, FGC: Filo Gris Complex, CMC: Choapa Metamorphic Complex, GC: Guarguaraz Complex, CCMC: Central Chile Metamorphic Complex. Terrane boundaries modified from Ramos (2009).

Upper Silurian − Early Devonian, homogenization event, and a Rb−Sr mineral isochron (246 ± 18 Ma) and two K−Ar ages (239 ± 0, muscovite; 236 ± 6 Ma, biotite) that may indicate a late-stage Triassic resetting (Ribba et al., 1988).

Other unit that have been considered as a candidate to be part of the Chilenia basement is the Las Yaretas Gneiss: a larger metasedimentary assemblage, associated with mafic sills, ultramafic bodies intruded by basaltic dikes (López de Azarevich et al., 2009) that appear at Cordón del Portillo in the Frontal Cordillera, SW of Mendoza (33°−34°S, Fig. 1). Two U/Pb conventional ages (1081 ± 45 Ma and 1069 ± 36 Ma) were reported by Ramos and Basei (1997) for the Las Yaretas Gneiss leading these authors to suggest a Laurentian ("Grenvillian") origin for the Chilenia terrane (Keppie and Ramos, 1999). Nevertheless, a recent paper by López de Azarevich et al. (2009) considers Las Yaretas Gneiss as slices of the Cuyania terrane basement that were tectonically incorporated within a subduction-related accretionary prism (the Guarguaraz Complex, see Massonne and Calderón, 2008; Willner et al., 2009a,b, 2011) that developed during the Devonian (ca. 390 Ma) along the eastern margin of the Chilenia Terrane (see below). More recently Astini and Cawood (2009) have described, in the Frontal Cordillera of La Rioja near Laguna Brava, further to the north (28°23′S−68°51′W, Fig. 1) a sequence of mottled phyllites and metagreywakes (Filo Gris Complex), intruded by Late Paleozoic leucogranites (U/Pb zircon SHRIMP age of 274 ± 2.7 Ma). Although the precise depositional age for these metasediments is unknown, the lack of any Early Middle Cambrian (Pampean), Ordovician (Famatinian), or younger age zircons, of common occurrence in nearby Late Paleozoic sedimentary sequences, lead them to suggest that some kind of paleogeographic barrier must have existed in order to prevent the supply of detrital zircons from sources on the Gondwana margin where such ages are thoroughly reported. Such relations support Astini and Cawood (2009) suggestion that the Filo Gris Complex represent part of a sedimentary blanket deposited on top of the Chilenia microplate before its final accretion to Gondwana.

In summary, most of the basement of Chilenia is unexposed probably because of the extensive cover of younger sediment and volcanic rocks and late Paleozoic batholiths that, at present, dominate the surface geology of the Frontal Cordillera both in Argentina and Chile. Despite these shortcomings, the nature of the Chilenia terrane can be interpreted by analyzing geological units exposed both along its eastern and western margins and formed by two contrasting accretionary prism systems, composed of continent-derived metasediments, including intercalations of disrupted oceanic crust that underwent HT/LP metamorphism.

The eastern unit comprises the already mentioned Guarguaraz Complex (Fig. 1). This metamorphic rock assemblage has been interpreted as an accretionary prism formed during closure of the oceanic space separating autochthonous Gondwana from the Chilenia microplate. Willner et al. (2008, 2009a,b, 2011) determined that peak HP/LT metamorphism occurred in the Mid-Devonian (390 ± 2 Ma, Lu−Hf mineral isochrons from metapelite and metabasite). Peak pressure conditions occurred at 1.40 GPa and 530 °C around a low metamorphic geotherm of 10−12 °C/km. According to Massonne and Calderón (2008) and Willner et al. (2011) metamorphic peak was followed by a decompression path with slight heating at 0.5 GPa at 560 °C following a clockwise P−T loop consistent with a continent−continent collisional scenario where Chilenia was probably part of the downgoing plate. A $^{40}Ar/^{39}Ar$ plateau age of white mica at 353 ± 1 Ma indicates the time of cooling below 350−400 °C. Fission track ages of zircons of 295 and 283 Ma record cooling below 280 °C (Willner et al., 2011).

The western accretionary complex form most of the large "metamorphic basement" of the Coastal Cordillera of central Chile, which south of 34°S reached peak HP−LT metamorphism in the Carboniferous (319−292 Ma, Willner et al., 2005, Fig. 1). Smaller and discontinuous outcrops occur further north along the coast between La Serena and Los Vilos (Choapa Metamorphic Complex, 30°−32°S, Fig. 1) and also in the coast of the Atacama region, near Vallenar, from 28° to 29°S (Huasco Metamorphic Complex,

Moscoso et al., 1982; Godoy and Wellkner, 2003; Welkner et al., 2006). A coeval magmatic arc, linked to east-directed subduction of the proto-Pacific oceanic crust that began after the docking of Chilenia to Gondwana is represented by large Upper Carboniferous to Lower Permian calc-alkaline plutons extending along the Frontal Cordillera between 27° and 32°S (i.e.: Elqui-Limarí, Chollay, Montosa and Collangüil batholiths (Mpodozis and Kay, 1992)). In north-central Chile metamorphic rocks occur, not only in the coastal region but also further inland at 28°40′S, in the El Tránsito valley (Fig. 2) where outcrops of a metamorphic complex, described by Ribba (1985) as the El Tránsito Metamorphic Complex (Fig. 1) appears a few kilometers to the west of the of the La Pampa Gneisses outcrops (Fig. 1). Although we cannot totally exclude of this being another relic of the Chilenia "basement", El Tránsito Metamorphic Complex was interpreted by Ribba et al. (1988), as part of the western Late Paleozoic accretionary prism.

Independently of the precise tectonic significance of the afore-mentioned metamorphic complexes in recent years the use of high-resolution dating of detrital zircon populations has become an important tool for determining the maximum age of deposition, tracing the source of detrital material in sedimentary and metamorphic units and refining knowledge of the tectonics and paleogeography of the Andean basement (Rapela et al., 2007; Willner et al., 2008, 2009a,b; Dahlquist et al., 2008; Collo et al., 2009; Bahlburg et al., 2009; Adams et al., 2008, 2010). In this contribution we present the results of the analysis of detrital zircon populations from samples collected in the El Tránsito Huasco and Choapa metamorphic complexes in order to narrow the maximum age of deposition, determine the nature of the detrital zircon populations, trace their potential sources and assess whether or not they provide information to support the existence of the Chilenia terrane.

2. El Tránsito, Huasco and Choapa Metamorphic Complexes

2.1. The El Tránsito Metamorphic Complex

The El Tránsito Metamorphic Complex outcrops along 8 km section of the El Tránsito valley to the east of Vallenar (Figs. 1 and 2). Both the El Tránsito Metamorphic Complex and La Pampa Gneisses are intruded by late Carboniferous to Permian plutons of the Elqui-Limarí Batholith (Ribba et al., 1988; Mpodozis and Kay, 1992). The El
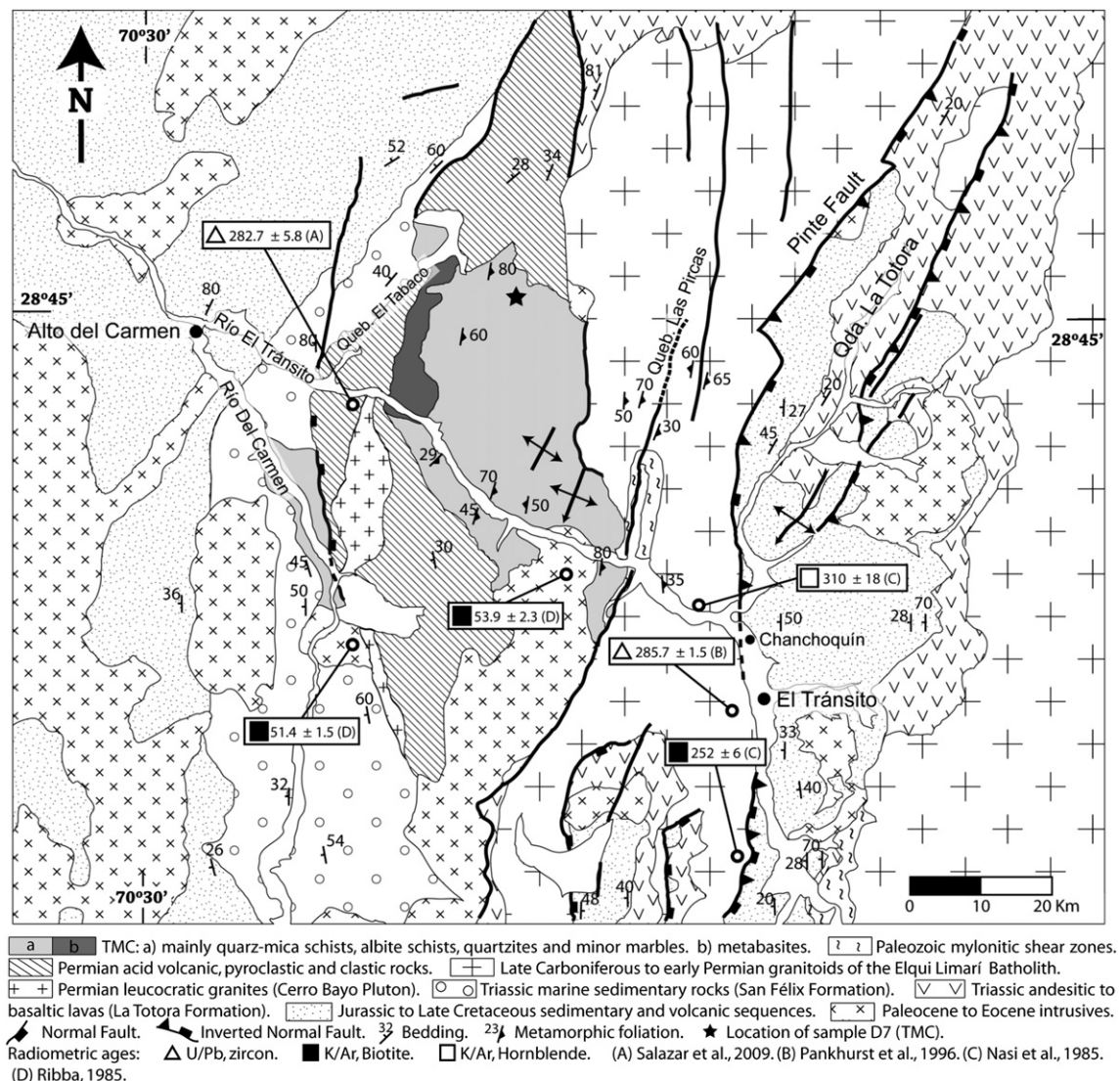

Fig. 2. Simplified geological map of the region of San Félix and El Tránsito valleys, to the east of Vallenar (III Region, Chile) showing lithologies of the El Tránsito Metamorphic Complex, location of sample D7, Late Paleozoic to Meso-Cenozoic cover successions and intrusive rocks and published radiometric ages.

Tránsito Metamorphic Complex is covered in angular unconformity and/or appear in tectonic contact with Permian leucocratic intrusives, Permian to Triassic volcanic sequences and Triassic conglomerates and greywackes (San Félix Formation) interpreted to have been deposited in a marine rift basin (Reutter, 1974; Ribba et al., 1988; Mpodozis and Cornejo, 1997; Salazar et al., 2009). The El Tránsito Metamorphic Complex includes greenschist, quartz–mica schist, albite nodular schist, quartzite and minor marble affected by, at least two superimposed deformation events. The earliest deformation (D1) is shown by a penetrative foliation (S1) that destroyed primary textures while the second deformation (D2) is associated to large-scale folding of the main foliation and to small-scale chevron folds, kink bands and a less penetrative cleavage (S2) (Ribba et al., 1988). Major and trace element geochemistry of the greenschists show strong affinities with ocean-floor basalts (MORB), whereas the geochemistry of quartz–mica schist and shale is consistent with a derivation from the erosion of intermediate to acidic igneous rocks (Ribba, 1985; Ribba et al., 1988). Mineralogical associations in the greenschist (albite + chlorite + epidote ± hornblende ± actinolite ± quartz ± calcite ± biotite), quartz–mica schist (albite + quartz + white mica ± biotite ± garnet ± chlorite) and marble (calcite ± scapolite ± tremolite ± biotite ± hornblende ± diopside ± wollastonite), together with mineral chemistry (amphibole in metabasite and white mica in metapelite) suggest intermediate P/T metamorphic conditions transitional between greenschist and amphibolite facies and pressures up to 5 Kbar during the main metamorphic event (Ribba et al., 1988).

The age of the El Tránsito Metamorphic Complex is not well constrained yet some poorly defined Rb/Sr whole rock Rb–Sr "errorchrons" (304 ± 40, 303 ± 40 and 335 ± 20 Ma) points to a main metamorphic episode during the Carboniferous (Ribba et al., 1988). Like in the La Pampa Gneiss, K/Ar muscovite ages (238 ± 10, 231 ± 6, 229 ± 6 Ma) indicate a Triassic cooling event also recorded by a 248 ± 46 Ma, Rb/Sr, whole rock, errorchron (Ribba et al., 1988).

2.2. The Huasco Metamorphic Complex

The Huasco Metamorphic Complex forms important outcrops along the coast of the Atacama Region between 27°S (Río Copiapó) and 29°S (Quebrada Los Choros, Fig. 1). The Huasco Metamorphic Complex is a petrotectonic assemblage of metasandstone, phyllite, quartzite and schist interleaved with lenses of marble, metachert and metabasalt showing in some places still well preserved pillow structures. Deformation is polyphasic and characterized by alternating bands of high- and low-strain. Most of the metasedimentary units are turbidites that were apparently deposited in a medial to distal submarine fan (Moscoso et al., 1982; Godoy and Wellkner, 2003; Welkner et al., 2006). The complex is overlain in angular unconformity by middle Triassic–early Jurassic sedimentary and volcanic strata (Canto del Agua Formation, Moscoso et al., 1982) and it is intruded by Triassic to middle Cretaceous batholiths. Welkner et al. (2006), based on regional correlations with units outcropping along the coast near Chañaral at 26°S (Las Tórtolas Formation, Bell, 1984, Fig. 1), suggested a possibly "Devonian to Lower Carboniferous" age while they indicate that sedimentation and metamorphism occurred before the accumulation of a fossiliferous, non-metamorphic, shallow water, marine platform carbonate and terrigenous Permian sedimentary sequence (Llano de Chocolate Strata). Interpreted as part of an accretionary prism complex (e.g. Bell, 1984) the Huasco Metamorphic Complex was affected by greenschist facies metamorphism and superimposed contact metamorphism in the vicinity of the Mesozoic plutons (Welkner et al., 2006).

2.3. The Choapa Metamorphic Complex

The Choapa Metamorphic Complex is composed of metamorphic rocks that occur discontinuously in the Coastal Cordillera of the Coquimbo Region between 31° and 32°S (Fig. 1). The most characteristic and more thoroughly studied outcrops of the Choapa Metamorphic Complex can be found north of Los Vilos between Quebrada El Teniente and Playa La Cebada (Irwin et al., 1988; Rivano and Sepulveda, 1991; Willner et al., 2008). At Playa La Cebada, the Choapa Metamorphic Complex is formed by metabasites of basaltic protolith, metachert, metasandstone and meta-conglomerate (Irwin et al., 1988) while further south near Los Vilos it includes quartz–mica schist, phyllite, schist amphibolite and marble (Rivano and Sepulveda, 1991). The Choapa Metamorphic Complex transitionally grades into a low-grade turbidite sequence with preserved sedimentary structures (Arrayán Formation) that, in turn, is uncomformably covered by the Huentelauquén Formation, a heterogeneous Upper Carboniferous to Permian sedimentary succession including platform limestone, conglomerate and shallow water clastic sediments (probably equivalent to the Llano de Chocolate Strata exposed in the coast of the Huasco region). According to Willner et al. (2008), both the Choapa Metamorphic Complex and the Arrayán Formation represent parts of an accretionary prism formed along the western margin of Chilenia in the late Paleozoic. Zircon fission track ages of 274 ± 18 Ma and 272 ± 40 Ma are considered as indicative of the age of peak metamorphism in the Choapa Metamorphic Complex, whereas Ar–Ar white mica ages are grouped at 248–199 Ma and 143–129 Ma. According to Willner et al. (2008) the latter represent ages that resetting event which "is assumed to be due to influx of fluids ascending in hydrothermal systems within extensional environments that have occurred from Upper Triassic to Jurassic times".

3. Detrital zircons: U/Pb geochronology

3.1. Analytical methods

In order to study the detrital zircon populations of the previously described three metamorphic complexes, we have collected one representative sample from each one. Zircons were separated from the hosting rocks using standard mineral separation in the Department of Geology at the Universidad de Chile. After crushing, reducing grain and sieving at <500 μm, zircon grains were separated using a Gemini Table, Frantz magnetic separation and heavy liquids (bromophorm and methylene iodide). Final zircon selection was carried out by hand-picking under a binocular microscope. U–Pb zircon ages were obtained using laser ablation inductively coupled plasma mass spectrometry (LA-ICP-MS) on mineral concentrate. About 100 zircon grains were then analyzed for each sample. U–Pb geochronology of zircons from samples of the Choapa Metamorphic Complex (sample LC03) and the El Tránsito Metamorphic Complex (sample D7) were conducted by laser ablation multicollector inductively coupled plasma mass spectrometry (LA-MC-ICP-MS) at the Arizona LaserChron Center (University of Arizona), whereas one sample (JA08) was analyzed by laser ablation inductively coupled plasma mass spectrometry (LA-ICP-MS) at the School Radiogenic Isotope and Geochronology Laboratory at Washington State University.

At the Arizona LaserChron Center, zircons crystals were analyzed with a Micromass Isoprobe multicollector ICPMS equipped with nine Faraday collectors, an axial Daly collector, and four ion-counting channels (Gehrels et al., 2008). The Isoprobe is equipped with an ArF Excimer laser ablation system, which has an emission wavelength of 193 nm. The collector configuration allows

measurement of ^{204}Pb in an ion-counting channel while ^{206}Pb, ^{207}Pb, ^{208}Pb, ^{232}Th and ^{238}U are simultaneously measured with Faraday detectors. All analyses were conducted in static mode with a laser beam diameter of 35 μm diameter, operated with an output energy of ∼32 mJ (at 23 kV) and a pulse rate of 8 Hz. Each analysis consisted of one 12-s integration on peaks with no laser firing and 21-s integrations on peaks with the laser firing. Hg contribution to the ^{204}Pb mass position was removed by subtracting on-peak background values. Inter-element fractionation was monitored by analyzing an in-house zircon standard (SL-2), which has a concordant ID-TIMS age of 563.5 ± 3.2 Ma (2σ) (Gehrels et al., 2008). This standard was analyzed once for every five unknowns. The lead isotopic ratios were corrected for common Pb, using the measured ^{204}Pb, assuming an initial Pb composition according to Stacey and Kramers (1975) and respective uncertainties of 1.0, 0.3 and 2.0 for ^{206}Pb/^{204}Pb, ^{207}Pb/^{204}Pb, and ^{208}Pb/^{204}Pb.

At the Radiogenic Isotope and Geochronology Laboratory, zircons from sample JA08 (Huasco Metamorphic Complex) were mounted in a 1-inch diameter epoxy puck that was ground and polished to expose the grains. Photomicrograph maps and CL (cathodoluminescence) images were used to characterize the internal features of zircons such as growth zones and inclusions and to provide a base map for recording laser spot locations. Zircon U−Pb analyses were performed using a New Wave UP-213 laser ablation system in conjunction with a ThermoFinnigan Element2 single collector double-focusing magnetic sector ICPMS in the Radiogenic Isotope and Geochronology Laboratory at Washington State University (USA) following the analytical procedures described in Chang et al. (2006). Fixed 30 μm diameter spots were used with a laser frequency of 10 Hz, being the ablated material delivered to the torch by He and Ar gas. Each analysis consisted of a short blank analysis followed by 300 sweeps through masses 204, 206, 207, 208, 232, 235, and 238, taking approximately 35 s.

For this study we used two zircon standards: Peixe, with an age of 564 Ma (Dickinson and Gehrels, 2003), and FC-1, with an age of 1099 Ma (Paces and Miller, 1993). During a session the standards were analyzed two to three times every 5−10 unknown analyses. U−Th−Pb isotopic data are given in Table 2.

Accordingly, the age probability plots (Ludwig, 2003) used in this study were constructed using the ^{206}Pb/^{238}U age for young (<1.0 Ga) zircons and the ^{206}Pb/^{207}Pb age for older (>1.0 Ga) grains. In old grains, ages with >30% discordance or >5% reverse discordance are considered unreliable and were not used. Also analyses with error greater than 10% were rejected. Analytical data of these samples are reported in Tables 1 and 2 on which uncertainties are at the 1-σ level, and include only measurement errors. These diagrams show each age and its uncertainty (for measurement error only) as a normal distribution, and sum all ages from a sample into a single curve.

4. Results

4.1. Sample D7. El Tránsito Metamorphic Complex

This sample is a lepidogranoblastic quartz−mica schist made up of 55% subhedral quartz crystals with wavy extinction (0.1−0.4 mm long), 30% of subhedral white-mica (0.1−1.2 mm), 15% subhedral alkali feldspar (0.2−0.5 mm) and biotite, garnet and chlorite; zircon is the main accessory phase. In this sample, a total of 97 individual detrital zircon grains were dated. (Table 1) Most of the analyzed zircon show regular internal zonation pattern characteristic of a magmatic origin (Corfu et al., 2003). The concordia diagram shows a high age dispersion ranging from c. 400 to 3000 Ma, most of them plotting on or close to the Concordia line (Fig. 3A). The relative probability plot of detrital zircon U−Pb ages (Fig. 5A) shows

values from Devonian to the Archean. Density plot distribution shows younger zircon groupings in the Devonian (n = 2: 380, 390 Ma) and Ordovician (n = 3; peak at 464 Ma). Cambrian zircon grains are among the more common and plot in three slightly different groups with peaks at 492 (n = 3) 504 (n = 4) and 535 Ma (n = 10). The largest subpopulation, however, is a late Neoproterozoic group that shows major peaks at 554 Ma (n = 14) and 569 Ma (n = 29). Within the large Neoproterozoic population minor peaks (Fig. 5A inset) are recognized at 596 Ma (n = 9), 626 Ma (n = 6), 662 Ma (n = 4) and 867 Ma (n = 3). A significant, Mesoproterozoic population is also present (n = 19) showing a peak at 1069 Ma. Additional Paleoproterozoic (∼1770 and ∼2030 Ma) and Archean (2722 Ma and 3028 Ma) single grains are also present indicating a protracted recycled geological record. The Th/U ratio ranges from 0.011 to 2.983. Fourty-one of the 97 analyzed zircon grains (42.27%) have values ≥0.5 (Table 1, Fig. 4).

4.2. Sample JA08. Huasco Metamorphic Complex

This sample corresponds to a granolepidoblastic phyllite made up of 70% subhedral quartz crystals with wavy extinction (0.05−0.3 mm long), 20% subhedral biotite (0.05−0.1 mm long), and 10% white mica (0.05−0.1 mm). Accessory minerals include zircon and opaque oxides. A total of 91 zircon grains were dated and values are quoted in Table 2. The Concordia diagram indicates that most of the analyzed zircon plot in the Concordia line, bracketing the interval c. 340−2000 Ma (Fig. 3B). The relative probability plot (Fig. 5B) indicates how age interval extends from Mississippian to late Paleoproterozoic. The youngest zircons are Mississippian (peak at 342 Ma, n = 3) while the largest group is early Ordovician (Tremadocian) in age (peak at 485 Ma, n = 9). The second largest zircon subpopulation is a late Neoproterozoic (Ediacaran) group that shows peaks at 540 Ma and 575 Ma. Older Neoproterozoic zircons (Cryogenian) form a small group (n = 2) at 658 Ma. Mesoproterozoic zircons are numerous with a peak at 1100 Ma and a subordinate one at 1300 Ma and 1425 Ma observed. Few Paleoproterozoic single grains are also present including 3 grains with a statistical maximum at 1992 Ma (Fig. 5B). The Th/U ratio ranges from 0.080 to 1.507. Fourty-two of the 91 analyzed zircons (46.15%) have values ≥0.5 (Table 2, Fig. 4).

4.3. Sample LC03. Choapa Metamorphic Complex

This sample is a granolepidoblastic paragneiss, comprising 55% of euhedral and subhedral quartz with wavy extinction (0.1−1.5 mm long crystals) and sutured edges; 25% subhedral white mica, (0.03−0.06 mm); 15% of subhedral alkali feldspar (0.4−1.8 mm); 5% of subhedral biotite (0.2−0.7 mm), partially replaced by chlorite, and zircon as the main accessory phase. In this sample, a total of 92 detrital zircons were selected for U/Pb geochronology (Table 1). In contrast with the other two analyzed samples, the Concordia diagram (Fig. 3C) shows highly scattered discordant U/Pb ages but the age interval between c. 400 and 1000 Ma is rather similar to the one observed in sample D7 (El Tránsito Metamorphic Complex). The relative probability plot (Fig. 5C) shows an age distribution pattern similar to sample D7, with detrital zircon ages clustered between the Mississippian and Archean. Like in sample JA08 from the Huasco Metamorphic Complex, the youngest analyzed zircon is Mississippian, (a single grain at 340 Ma). In LC03 two grains with a statistical peak at 369 Ma (Fig. 5C). As in the other two samples the density plot also shows an important Ordovician population with peaks at 452 Ma (n = 7) and 484 Ma (n = 6). Like in the El Tránsito Metamorphic Complex sample, the largest age group is Neoproterozoic, within which the statistical discrimination allowed groupings with peaks

Table 1
LA-ICP-MS U–Pb zircon data for samples from the El Tránsito (TMC) and Choapa (CMC) Metamorphic Complexes.

Sample	Concentration			Isotope ratios							Apparent ages (Ma)					
	U (ppm)	Th (ppm)	U/Th	$\frac{^{206}Pb}{^{207}Pb}$	± (%)	$\frac{^{207}Pb}{^{235}U}$	± (%)	$\frac{^{206}Pb}{^{238}U}$	± (%)	Error corr.	$\frac{^{206}Pb}{^{238}U}$	± (Ma)	$\frac{^{207}Pb}{^{235}U}$	± (Ma)	$\frac{^{206}Pb}{^{207}Pb}$	± (Ma)
TMC: sample D7																
D7-1	436	157	2.8	9.17	3.94	4.082	4.10	0.2715	1.12	0.27	1548.6	15.4	1650.8	33.4	1783.5	71.9
D7-2	300	185	1.6	16.85	3.95	0.709	4.03	0.0866	0.82	0.20	535.4	4.2	544.0	17.0	579.9	85.8
D7-3	274	59	4.6	17.08	1.90	0.757	2.03	0.0937	0.71	0.35	577.5	3.9	572.1	8.9	550.8	41.5
D7-4	913	10	88.4	16.20	2.30	0.784	3.02	0.0921	1.95	0.65	568.0	10.6	587.9	13.5	665.4	49.3
D7-5	459	51	9.0	17.05	1.51	0.746	2.19	0.0923	1.59	0.72	568.8	8.7	566.0	9.5	554.7	33.0
D7-6	27	41	0.7	15.89	15.70	0.769	15.99	0.0887	3.04	0.19	547.7	16.0	579.3	70.7	705.6	335.9
D7-7	78	21	3.6	17.19	6.63	0.643	6.81	0.0801	1.57	0.23	496.9	7.5	504.0	27.1	536.6	145.3
D7-8	545	145	3.7	16.29	2.46	0.799	4.67	0.0944	3.97	0.85	581.4	22.1	596.3	21.1	653.3	52.8
D7-9	513	336	1.5	8.14	3.01	5.922	3.37	0.3498	1.52	0.45	1933.4	25.4	1964.5	29.3	1997.3	43.5
D7-10	484	117	4.1	14.53	3.12	1.132	3.59	0.1193	1.78	0.50	726.6	12.2	768.9	19.4	893.9	64.2
D7-13	570	85	6.7	16.81	4.06	0.781	4.11	0.0952	0.63	0.15	586.5	3.5	586.1	18.3	584.7	88.2
D7-14	883	37	23.8	16.73	3.04	0.756	3.13	0.0918	0.75	0.24	565.9	4.1	571.9	13.7	595.7	65.9
D7-15	275	257	1.1	16.00	2.27	0.987	2.39	0.1146	0.74	0.31	699.4	4.9	697.3	12.0	690.6	48.4
D7-16	183	341	0.5	16.99	3.52	0.686	3.67	0.0845	1.04	0.28	523.1	5.2	530.3	15.1	561.3	76.6
D7-17	254	12	20.4	18.20	4.53	0.562	4.58	0.0742	0.64	0.14	461.6	2.9	453.1	16.7	410.3	101.5
D7-19	59	39	1.5	17.07	6.75	0.704	7.19	0.0872	2.48	0.35	539.1	12.8	541.4	30.2	551.0	147.4
D7-20	135	30	4.4	12.54	4.12	2.152	4.16	0.1958	0.58	0.14	1152.5	6.1	1165.7	28.9	1190.5	81.4
D7-21	105	39	2.7	13.23	2.95	1.777	3.58	0.1705	2.03	0.57	1014.6	19.1	1036.9	23.3	1084.3	59.2
D7-22	341	160	2.1	13.20	2.20	1.954	2.43	0.1871	1.03	0.42	1105.5	10.5	1099.7	16.3	1088.4	44.1
D7-23	176	81	2.2	13.21	2.51	1.725	2.76	0.1653	1.14	0.41	986.1	10.4	1018.0	17.7	1087.2	50.4
D7-24	535	306	1.7	17.70	2.93	0.585	2.99	0.0750	0.58	0.19	466.4	2.6	467.5	11.2	472.6	64.9
D7-25	122	168	0.7	17.38	4.77	0.734	4.83	0.0926	0.73	0.15	570.7	4.0	559.1	20.8	512.1	105.0
D7-26	296	82	3.6	17.67	5.86	0.618	5.91	0.0791	0.78	0.13	491.0	3.7	488.3	22.9	475.9	129.7
D7-27	296	154	1.9	17.23	6.59	0.500	6.62	0.0625	0.62	0.09	390.8	2.4	411.9	22.4	531.9	144.5
D7-28	429	80	5.4	16.67	2.04	0.768	2.56	0.0928	1.55	0.60	572.3	8.5	578.5	11.3	603.0	44.2
D7-29	648	186	3.5	13.18	2.17	1.906	2.47	0.1822	1.18	0.48	1079.0	11.7	1083.1	16.5	1091.3	43.5
D7-30	455	156	2.9	11.95	2.50	1.883	3.18	0.1633	1.96	0.62	974.9	17.7	1075.2	21.1	1284.7	48.7
D7-32	87	86	1.0	5.44	2.89	12.444	3.68	0.4909	2.27	0.62	2574.4	48.2	2638.5	34.6	2688.1	47.8
D7-33	161	149	1.1	18.03	4.53	0.623	4.58	0.0815	0.65	0.14	505.1	3.2	491.9	17.9	430.9	101.1
D7-34	143	130	1.1	10.93	4.03	3.143	4.17	0.2491	1.07	0.26	1433.7	13.8	1443.2	32.1	1457.3	76.7
D7-36	234	129	1.8	16.07	2.06	0.908	2.23	0.1058	0.86	0.39	648.4	5.3	656.1	10.8	682.4	44.0
D7-38	91	44	2.1	13.37	4.08	1.878	4.12	0.1821	0.60	0.15	1078.2	6.0	1073.4	27.3	1063.6	82.1
D7-39	164	178	0.9	13.47	5.02	1.469	5.87	0.1435	3.03	0.52	864.4	24.5	917.6	35.5	1047.8	101.4
D7-40	83	45	1.8	16.78	2.54	0.759	3.08	0.0924	1.74	0.57	569.8	9.5	573.6	13.5	588.9	55.1
D7-41	160	47	3.4	17.50	1.67	0.679	2.14	0.0861	1.34	0.63	532.7	6.9	526.1	8.8	497.6	36.7
D7-43	202	186	1.1	15.96	2.02	0.948	2.49	0.1097	1.45	0.58	671.0	9.2	677.0	12.3	696.9	43.1
D7-44	381	198	1.9	12.81	2.32	1.890	2.76	0.1756	1.49	0.54	1043.1	14.4	1077.7	18.3	1148.4	46.1
D7-45	214	60	3.6	13.85	2.18	1.716	2.40	0.1724	1.01	0.42	1025.4	9.6	1014.6	15.4	991.4	44.4
D7-46	102	85	1.2	6.67	2.83	8.818	2.88	0.4268	0.54	0.19	2291.2	10.4	2319.3	26.3	2344.1	48.4
D7-47	879	101	8.7	16.93	2.64	0.741	3.89	0.0909	2.86	0.73	561.0	15.4	562.8	16.8	569.8	57.5
D7-48	852	272	3.1	16.59	1.23	0.809	1.59	0.0973	1.01	0.63	598.4	5.8	601.7	7.2	614.1	26.6
D7-49	197	301	0.7	16.82	1.58	0.812	2.01	0.0990	1.23	0.61	608.6	7.1	603.3	9.1	583.6	34.4
D7-50	145	101	1.4	17.58	3.14	0.674	3.58	0.0860	1.72	0.48	531.5	8.8	523.2	14.6	487.0	69.2
D7-51	743	464	1.6	16.27	1.53	0.920	1.90	0.1085	1.12	0.59	664.3	7.1	662.2	9.2	655.0	32.8
D7-52	339	134	2.5	18.50	3.43	0.453	3.53	0.0607	0.81	0.23	380.2	3.0	379.2	11.2	373.1	77.3
D7-53	67	60	1.1	8.93	4.12	5.086	4.19	0.3293	0.77	0.18	1834.9	12.3	1833.8	35.6	1832.5	74.7
D7-54	187	260	0.7	17.41	2.57	0.699	2.68	0.0883	0.74	0.28	545.5	3.9	538.6	11.2	508.6	56.6
D7-56	226	201	1.1	9.36	1.79	3.887	3.65	0.2640	3.18	0.87	1510.0	42.8	1611.0	29.5	1745.6	32.8
D7-57	179	86	2.1	4.49	2.67	17.697	3.27	0.5764	1.88	0.58	2933.9	44.3	2973.4	31.4	3000.2	42.9
D7-58	479	35	13.8	13.64	3.16	1.579	4.00	0.1562	2.45	0.61	935.7	21.3	962.0	24.9	1022.7	64.0
D7-60	86	118	0.7	18.09	7.00	0.662	7.19	0.0869	1.62	0.23	537.1	8.3	516.0	29.1	423.8	156.4
D7-61	298	124	2.4	13.35	2.70	1.845	2.91	0.1786	1.09	0.37	1059.5	10.6	1061.6	19.2	1065.9	54.3
D7-62	590	326	1.8	12.54	2.45	2.203	2.66	0.2003	1.03	0.39	1177.1	11.1	1181.8	18.6	1190.6	48.4
D7-63	400	79	5.1	16.08	2.44	0.946	2.60	0.1103	0.91	0.35	674.5	5.8	675.9	12.9	680.6	52.2
D7-64	1112	15	72.0	15.61	3.42	0.955	3.46	0.1081	0.50	0.14	662.0	3.1	680.8	17.1	743.6	72.3
D7-66	365	24	15.5	16.96	2.60	0.705	2.74	0.0868	0.85	0.31	536.3	4.4	541.9	11.5	565.2	56.7
D7-67	146	80	1.8	17.95	4.95	0.685	5.03	0.0891	0.91	0.18	550.3	4.8	529.6	20.8	441.1	110.1
D7-68	25	13	2.0	11.43	7.10	2.564	7.28	0.2125	1.59	0.22	1242.2	18.0	1290.4	53.2	1371.4	136.8
D7-69	188	70	2.7	4.39	2.79	17.701	3.10	0.5640	1.34	0.43	2883.2	31.2	2973.6	29.8	3035.4	44.7
D7-70	65	64	1.0	13.73	3.81	1.694	3.86	0.1687	0.62	0.16	1004.9	5.8	1006.4	24.7	1009.7	77.3
D7-71	357	7	51.1	12.25	2.56	2.305	2.72	0.2049	0.91	0.33	1201.4	10.0	1213.8	19.2	1236.0	50.2
D7-72	315	207	1.5	16.81	2.19	0.791	2.74	0.0964	1.64	0.60	593.1	9.3	591.6	12.3	585.5	47.6
D7-73	112	41	2.7	17.77	4.05	0.666	4.16	0.0858	0.97	0.23	530.4	4.9	518.0	16.9	463.8	89.7
D7-74	168	138	1.2	5.39	1.83	11.039	4.17	0.4316	3.75	0.90	2313.0	72.9	2526.4	38.9	2702.6	30.2
D7-76	226	50	4.5	16.25	3.98	0.800	4.68	0.0943	2.46	0.53	581.1	13.7	597.1	21.1	658.0	85.4
D7-77	80	31	2.5	13.67	3.54	1.787	3.62	0.1772	0.76	0.21	1051.5	7.4	1040.6	23.6	1017.8	71.8
D7-78	465	116	4.0	13.52	2.74	1.701	2.79	0.1667	0.50	0.18	994.0	4.6	1008.8	17.8	1041.1	55.3
D7-79	310	81	3.8	13.18	2.82	1.965	2.86	0.1878	0.50	0.17	1109.6	5.1	1103.6	19.3	1091.8	56.5
D7-80	609	130	4.7	16.45	1.61	0.867	1.74	0.1034	0.67	0.38	634.4	4.0	633.8	8.2	631.9	34.7
D7-81	341	84	4.1	16.50	2.91	0.811	3.02	0.0971	0.80	0.26	597.3	4.6	603.3	13.7	625.7	62.8

Table 1 (*continued*)

Sample	Concentration			Isotope ratios							Apparent ages (Ma)					
	U (ppm)	Th (ppm)	U/Th	$\frac{^{206}Pb}{^{207}Pb}$	± (%)	$\frac{^{207}Pb}{^{235}U}$	± (%)	$\frac{^{206}Pb}{^{238}U}$	± (%)	Error corr.	$\frac{^{206}Pb}{^{238}U}$	± (Ma)	$\frac{^{207}Pb}{^{235}U}$	± (Ma)	$\frac{^{206}Pb}{^{207}Pb}$	± (Ma)
D7-82	431	154	2.8	16.51	1.83	0.850	1.90	0.1018	0.50	0.26	625.1	3.0	624.8	8.9	623.6	39.5
D7-83	267	75	3.6	16.00	1.95	0.881	2.26	0.1022	1.13	0.50	627.3	6.8	641.5	10.7	691.8	41.7
D7-85	330	128	2.6	15.56	2.83	1.138	2.94	0.1284	0.78	0.27	778.8	5.7	771.6	15.9	750.7	59.8
D7-86	194	57	3.4	13.57	1.72	1.772	1.93	0.1744	0.88	0.46	1036.2	8.4	1035.3	12.5	1033.4	34.8
D7-87	125	65	1.9	13.36	2.29	1.885	2.38	0.1827	0.66	0.28	1081.9	6.6	1075.9	15.8	1063.9	46.1
D7-88	274	96	2.9	13.26	1.67	1.576	1.98	0.1516	1.07	0.54	909.9	9.1	960.8	12.3	1079.3	33.5
D7-89	829	244	3.4	16.62	3.10	0.780	3.16	0.0940	0.62	0.20	579.1	3.4	585.4	14.0	610.0	66.9
D7-90	1677	504	3.3	17.38	2.19	0.643	2.40	0.0811	0.99	0.41	502.6	4.8	504.2	9.6	511.7	48.1
D7-91	25	1	18.6	18.81	16.86	0.671	16.92	0.0916	1.39	0.08	564.8	7.5	521.4	69.1	335.4	384.6
D7-92	347	127	2.7	13.26	1.77	1.783	2.21	0.1715	1.33	0.60	1020.2	12.5	1039.2	14.4	1079.4	35.5
D7-93	345	142	2.4	16.22	1.86	0.890	2.51	0.1047	1.68	0.67	641.9	10.3	646.5	12.0	662.6	39.9
D7-94	71	211	0.3	8.03	2.00	6.124	2.41	0.3567	1.34	0.56	1966.5	22.7	1993.7	21.0	2021.9	35.5
D7-95	293	125	2.4	13.73	1.91	1.596	3.49	0.1590	2.92	0.84	951.3	25.8	968.8	21.8	1008.7	38.7
D7-96	818	45	18.2	15.06	1.82	1.139	1.89	0.1244	0.50	0.26	755.8	3.6	772.0	10.2	819.2	38.0
D7-97	202	103	2.0	17.01	1.54	0.747	2.22	0.0922	1.59	0.72	568.6	8.7	566.7	9.6	559.2	33.7
D7-98	283	107	2.6	16.87	2.86	0.796	3.19	0.0974	1.41	0.44	599.0	8.1	594.4	14.4	576.6	62.2
D7-99	1062	100	10.6	16.25	2.76	0.869	2.81	0.1025	0.53	0.19	628.8	3.2	635.1	13.3	657.7	59.2
D7-100	224	139	1.6	17.45	4.32	0.691	4.52	0.0874	1.32	0.29	540.3	6.8	533.2	18.7	502.8	95.2
D7-101	628	86	7.3	16.46	1.96	0.848	2.04	0.1013	0.58	0.28	622.0	3.4	623.8	9.5	630.3	42.2
D7-102	174	34	5.2	16.19	4.34	0.799	5.44	0.0938	3.28	0.60	578.2	18.1	596.3	24.6	665.7	93.1
D7-103	225	89	2.5	13.76	2.17	1.446	5.29	0.1443	4.82	0.91	869.0	39.2	908.1	31.7	1004.3	44.1
D7-104	394	114	3.4	16.67	3.94	0.653	5.62	0.0790	4.01	0.71	490.1	18.9	510.5	22.6	603.0	85.3
D7-105	244	98	2.5	5.36	1.05	12.569	4.15	0.4884	4.01	0.97	2563.8	84.8	2647.9	39.0	2712.8	17.3
D7-106	167	478	0.3	16.95	2.87	0.786	2.94	0.0966	0.65	0.22	594.7	3.7	588.9	13.1	566.7	62.4
D7-107	564	166	3.4	17.19	2.20	0.720	2.26	0.0898	0.50	0.22	554.1	2.7	550.6	9.6	535.9	48.1
D7-109	839	417	2.0	17.83	1.62	0.540	1.91	0.0699	1.00	0.52	435.3	4.2	438.5	6.8	455.3	36.0
D7-110	323	83	3.9	14.16	2.26	1.244	3.09	0.1277	2.10	0.68	774.8	15.3	820.6	17.4	947.0	46.3
CMC: sample LC03																
LC03-1	6	3	2.0	17.24	27.86	0.534	29.04	0.0667	8.19	0.28	416.3	33.0	434.2	103.0	530.4	621.5
LC03-2	395	234	1.7	12.56	0.74	2.024	0.91	0.1843	0.53	0.58	1090.2	5.3	1123.5	6.2	1188.3	14.7
LC03-3	476	184	2.6	16.13	1.26	0.921	1.82	0.1078	1.31	0.72	659.8	8.2	662.9	8.9	673.5	27.0
LC03-4	119	5	22.1	16.01	10.98	0.783	11.03	0.0909	1.04	0.09	560.7	5.6	587.1	49.2	690.5	234.8
LC03-6	773	116	6.6	6.01	0.85	9.258	1.03	0.4035	0.58	0.56	2185.0	10.7	2363.9	9.4	2522.0	14.3
LC03-7	284	51	5.6	11.92	1.28	2.318	2.17	0.2004	1.75	0.81	1177.2	18.8	1217.8	15.4	1290.3	24.9
LC03-8	521	130	4.0	13.12	1.19	1.774	2.15	0.1688	1.79	0.83	1005.7	16.7	1035.9	14.0	1100.3	23.8
LC03-9	323	110	2.9	13.93	3.00	1.423	3.11	0.1438	0.83	0.27	865.9	6.7	898.6	18.6	979.7	61.1
LC03-10	166	73	2.3	5.43	1.02	10.784	1.24	0.4250	0.70	0.57	2283.0	13.5	2504.7	11.5	2689.7	16.9
LC03-11	523	31	16.8	16.84	0.90	0.781	1.21	0.0954	0.81	0.67	587.3	4.5	586.0	5.4	581.2	19.6
LC03-12	124	59	2.1	12.98	3.00	1.923	3.74	0.1810	2.23	0.60	1072.6	22.0	1089.1	25.0	1122.3	59.8
LC03-13	97	65	1.5	18.27	4.38	0.580	5.31	0.0769	2.99	0.56	477.6	13.8	464.7	19.8	401.4	98.2
LC03-14	29	25	1.2	19.29	19.32	0.578	20.85	0.0809	7.83	0.38	501.3	37.8	463.1	77.7	278.1	446.0
LC03-15	823	94	8.7	16.42	1.26	0.888	2.21	0.1058	1.81	0.82	648.3	11.2	645.4	10.5	635.3	27.1
LC03-16	761	9	86.5	16.61	0.75	0.808	1.28	0.0973	1.04	0.81	598.8	5.9	601.3	5.8	610.6	16.2
LC03-17	304	106	2.9	16.83	1.04	0.750	2.14	0.0915	1.87	0.87	564.5	10.1	568.1	9.3	582.6	22.6
LC03-18	203	195	1.0	13.49	0.92	1.590	2.20	0.1555	2.00	0.91	931.6	17.3	966.1	13.7	1045.6	18.6
LC03-19	627	187	3.4	13.90	1.80	1.691	1.90	0.1705	0.62	0.33	1014.8	5.8	1005.3	12.2	984.5	36.6
LC03-20	377	202	1.9	13.32	0.74	1.886	1.55	0.1822	1.36	0.88	1078.8	13.5	1076.2	10.3	1071.1	14.9
LC03-21	785	72	10.9	15.61	0.70	1.098	0.99	0.1243	0.70	0.71	755.1	5.0	752.2	5.3	743.5	14.8
LC03-22	243	68	3.6	16.31	10.47	0.780	10.54	0.0922	1.22	0.12	568.8	6.6	585.5	46.9	650.6	225.4
LC03-23	333	344	1.0	16.56	1.91	0.861	2.23	0.1034	1.14	0.51	634.2	6.9	630.5	10.5	617.4	41.3
LC03-24	137	73	1.9	17.06	3.51	0.765	3.73	0.0947	1.25	0.34	583.1	7.0	576.9	16.4	552.6	76.6
LC03-25	181	136	1.3	13.23	1.08	1.901	2.22	0.1824	1.94	0.87	1080.0	19.3	1081.5	14.8	1084.5	21.7
LC03-27	732	54	13.6	13.65	1.66	1.727	2.27	0.1710	1.55	0.68	1017.4	14.6	1018.8	14.6	1021.8	33.6
LC03-28	862	379	2.3	17.06	0.81	0.719	1.52	0.0890	1.28	0.84	549.3	6.7	550.1	6.4	553.0	17.7
LC03-30	458	410	1.1	17.89	1.60	0.597	2.16	0.0774	1.45	0.67	480.7	6.7	475.2	8.2	448.6	35.7
LC03-31	766	120	6.4	16.13	1.30	0.841	1.39	0.0983	0.50	0.36	604.7	2.9	619.6	6.5	674.3	27.8
LC03-32	120	77	1.6	16.81	3.76	0.685	4.30	0.0835	2.09	0.49	517.2	10.4	530.0	17.8	585.6	81.7
LC03-33	564	254	2.2	14.06	0.92	1.462	1.05	0.1490	0.50	0.48	895.6	4.2	914.8	6.3	961.5	18.8
LC03-34	255	366	0.7	8.94	1.57	3.418	5.30	0.2216	5.06	0.96	1290.3	59.2	1508.6	41.6	1830.0	28.5
LC03-35	459	325	1.4	12.92	3.65	1.553	4.12	0.1455	1.92	0.47	875.9	15.7	951.7	25.5	1131.5	72.6
LC03-36	541	235	2.3	13.66	1.42	1.714	1.95	0.1699	1.33	0.68	1011.5	12.5	1013.9	12.5	1019.2	28.8
LC03-37	61	36	1.7	16.52	2.50	0.740	2.70	0.0887	1.01	0.37	547.7	5.3	562.5	11.7	623.0	54.0
LC03-38	1218	56	21.6	16.76	1.02	0.784	2.82	0.0953	2.63	0.93	586.7	14.7	587.7	12.6	591.4	22.1
LC03-39	163	97	1.7	18.89	2.32	0.422	2.48	0.0579	0.89	0.36	362.6	3.1	357.6	7.5	325.8	52.6
LC03-40	188	69	2.7	13.93	2.25	1.146	3.07	0.1157	2.09	0.68	706.0	14.0	775.2	16.7	980.1	45.9
LC03-41	431	30	14.4	13.41	1.59	1.668	2.27	0.1622	1.62	0.71	969.3	14.6	996.3	14.4	1056.4	32.0
LC03-42	305	131	2.3	18.32	2.55	0.444	2.61	0.0590	0.52	0.20	369.7	1.9	373.2	8.1	395.0	57.3
LC03-43	514	28	18.1	16.42	2.46	0.811	3.69	0.0966	2.75	0.75	594.6	15.6	603.3	16.8	636.0	53.0
LC03-44	341	30	11.3	17.12	2.03	0.586	2.09	0.0727	0.50	0.24	452.3	2.2	468.0	7.8	545.6	44.3
LC03-45	180	193	0.9	16.68	4.77	0.727	4.82	0.0879	0.68	0.14	543.4	3.5	554.8	20.6	601.8	103.3
LC03-46	165	114	1.4	16.45	2.55	0.872	3.48	0.1037	2.37	0.68	635.8	14.3	636.5	16.5	638.8	54.9
LC03-47	46	15	3.2	16.25	3.01	0.932	3.40	0.1099	1.58	0.46	672.2	10.1	668.9	16.7	657.9	64.6
LC03-48	243	132	1.8	13.82	3.32	1.443	8.60	0.1447	7.93	0.92	870.9	64.6	906.8	51.6	995.3	67.5

Table 1 (continued)

Sample	Concentration			Isotope ratios							Apparent ages (Ma)					
	U (ppm)	Th (ppm)	U/Th	$\frac{206Pb}{207Pb}$	± (%)	$\frac{207Pb}{235U}$	± (%)	$\frac{206Pb}{238U}$	± (%)	Error corr.	$\frac{206Pb}{238U}$	± (Ma)	$\frac{207Pb}{235U}$	± (Ma)	$\frac{206Pb}{207Pb}$	± (Ma)
LC03-49	354	44	8.1	17.08	2.30	0.726	2.47	0.0899	0.90	0.36	554.8	4.8	553.9	10.6	550.3	50.3
LC03-520	137	41	3.3	6.63	1.35	8.966	2.11	0.4313	1.62	0.77	2311.4	31.5	2334.6	19.3	2354.9	23.1
LC03-51	195	83	2.4	17.24	1.63	0.711	2.15	0.0889	1.41	0.65	549.1	7.4	545.5	9.1	530.6	35.7
LC03-52	236	157	1.5	6.10	1.58	9.763	2.55	0.4318	2.00	0.78	2314.0	38.9	2412.7	23.5	2497.0	26.6
LC03-53	706	264	2.7	14.31	2.25	1.126	2.49	0.1169	1.05	0.42	712.5	7.1	766.0	13.4	925.5	46.3
LC03-54	696	149	4.7	14.00	1.60	1.362	2.51	0.1383	1.93	0.77	834.8	15.1	872.7	14.7	970.2	32.7
LC03-55	137	70	2.0	11.54	3.05	2.156	10.40	0.1805	9.94	0.96	1069.5	98.0	1167.0	72.2	1352.9	58.9
LC03-56	490	95	5.2	14.95	1.51	1.055	1.64	0.1144	0.64	0.39	698.1	4.2	731.1	8.6	833.7	31.5
LC03-57	840	242	3.5	5.13	2.41	13.563	2.46	0.5049	0.50	0.20	2634.8	10.8	2719.7	23.3	2783.4	39.5
LC03-58	437	70	6.2	13.93	2.21	1.271	3.32	0.1284	2.48	0.75	778.9	18.2	833.1	18.9	980.3	45.1
LC03-59	441	17	25.6	4.77	2.76	14.697	3.00	0.5089	1.18	0.39	2652.1	25.7	2795.8	28.5	2901.3	44.8
LC03-60	242	44	5.6	16.26	1.23	0.787	4.57	0.0929	4.40	0.96	572.6	24.1	589.7	20.4	656.3	26.3
LC03-61	196	93	2.1	14.15	2.08	1.265	2.20	0.1299	0.69	0.31	787.0	5.1	830.3	12.5	947.8	42.7
LC03-62	609	77	7.9	16.46	1.45	0.771	1.54	0.0920	0.50	0.33	567.4	2.7	580.1	6.8	630.5	31.3
LC03-63	375	134	2.8	15.94	2.76	0.798	2.81	0.0922	0.50	0.18	568.7	2.7	595.6	12.6	699.6	58.8
LC03-64	1436	185	7.8	16.38	1.13	0.861	1.93	0.1023	1.56	0.81	627.7	9.3	630.4	9.0	640.4	24.3
LC03-65	166	79	2.1	8.83	1.79	4.626	3.13	0.2964	2.57	0.82	1673.4	37.9	1753.9	26.2	1851.2	32.4
LC03-66	535	200	2.7	13.12	1.45	1.771	1.65	0.1685	0.79	0.48	1004.0	7.3	1034.9	10.7	1100.8	29.0
LC03-67	162	155	1.0	17.40	2.06	0.692	2.18	0.0873	0.71	0.33	539.5	3.7	533.8	9.0	509.6	45.2
LC03-68	170	96	1.8	10.81	1.01	3.072	1.65	0.2408	1.30	0.79	1391.1	16.3	1425.7	12.6	1477.8	19.2
LC03-69	211	34	6.2	17.14	2.28	0.683	3.06	0.0848	2.04	0.67	525.0	10.3	528.4	12.6	543.2	49.8
LC03-72	190	87	2.2	13.08	3.47	1.677	8.11	0.1591	7.33	0.90	951.7	64.9	1000.0	51.6	1107.4	69.3
LC03-73	119	63	1.9	5.62	1.33	10.765	1.42	0.4386	0.50	0.35	2344.4	9.8	2503.0	13.2	2634.4	22.1
LC03-74	394	184	2.1	8.10	4.34	4.940	4.66	0.2902	1.71	0.37	1642.6	24.8	1809.0	39.4	2006.6	77.1
LC03-75	98	134	0.7	13.51	3.60	1.689	3.77	0.1654	1.12	0.30	986.8	10.2	1004.3	24.0	1042.6	72.6
LC03-76	421	143	2.9	12.00	2.04	2.045	2.12	0.1780	0.56	0.26	1056.3	5.5	1130.6	14.4	1276.2	39.8
LC03-78	95	239	0.4	16.88	6.88	0.688	8.67	0.0842	5.27	0.61	521.0	26.4	531.3	35.9	575.8	149.8
LC03-77	484	284	1.7	15.14	13.70	0.717	13.75	0.0788	1.11	0.08	488.8	5.2	549.2	58.4	807.9	288.0
LC03-79	200	128	1.6	16.69	1.73	0.812	2.08	0.0983	1.16	0.56	604.2	6.7	603.5	9.5	600.6	37.5
LC03-80	65	95	0.7	18.14	3.66	0.533	4.35	0.0702	2.34	0.54	437.1	9.9	434.0	15.4	417.5	81.8
LC03-81	681	61	11.2	16.61	1.32	0.719	2.22	0.0866	1.78	0.80	535.1	9.1	549.9	9.4	611.4	28.6
LC03-82	199	168	1.2	10.57	7.94	2.584	8.56	0.1981	3.18	0.37	1164.9	33.9	1296.0	62.7	1520.2	150.0
LC03-85	257	14	17.8	5.62	2.86	8.916	9.57	0.3634	9.13	0.95	1998.5	156.9	2329.5	87.6	2633.6	47.5
LC03-86	238	85	2.8	7.02	1.22	8.068	1.53	0.4106	0.93	0.61	2217.5	17.4	2238.6	13.9	2258.0	21.1
LC03-87	211	200	1.1	16.69	3.10	0.773	3.22	0.0936	0.85	0.26	576.7	4.7	581.6	14.2	600.5	67.2
LC03-88	535	179	3.0	17.71	1.93	0.607	2.09	0.0779	0.79	0.38	483.7	3.7	481.4	8.0	470.3	42.8
LC03-89	390	105	3.7	14.17	2.90	1.267	3.99	0.1302	2.74	0.69	789.3	20.4	831.2	22.7	944.9	59.4
LC03-90	295	118	2.5	16.56	11.52	0.742	11.56	0.0891	0.98	0.08	550.3	5.2	563.4	50.0	617.0	249.5
LC03-91	323	125	2.6	16.46	2.36	0.877	2.41	0.1047	0.50	0.21	641.7	3.1	639.3	11.4	630.6	50.8
LC03-92	350	84	4.2	14.71	1.19	1.163	1.59	0.1240	1.05	0.66	753.8	7.5	783.2	8.7	868.1	24.7
LC03-94	860	346	2.5	14.11	1.14	1.106	1.95	0.1131	1.58	0.81	690.9	10.4	756.1	10.4	953.9	23.3
LC03-95	226	418	0.5	15.55	6.23	0.479	6.39	0.0540	1.40	0.22	339.3	4.6	397.4	21.0	751.3	131.7
LC03-96	414	165	2.5	17.85	1.53	0.591	2.44	0.0765	1.90	0.78	475.1	8.7	471.4	9.2	453.2	34.0
LC03-97	163	93	1.7	12.60	5.70	2.036	6.08	0.1860	2.12	0.35	1099.5	21.4	1127.5	41.4	1181.8	112.7
LC03-98	440	566	0.8	17.24	6.58	0.578	6.64	0.0723	0.88	0.13	449.9	3.8	463.3	24.7	530.6	144.3
LC03-99	202	133	1.5	6.35	3.03	8.516	4.41	0.3921	3.21	0.73	2132.4	58.3	2287.7	40.1	2429.4	51.4
LC03-100	154	152	1.0	17.21	2.11	0.698	2.54	0.0871	1.41	0.56	538.3	7.3	537.5	10.6	534.1	46.1

at 545 Ma ($n = 14$), 568 Ma ($n = 11$), 604 ($n = 6$), 642 ($n = 5$), 659 ($n = 4$), 698 ($n = 3$), 711 ($n = 3$), 755 ($n = 5$) and 787 Ma ($n = 4$). Older single grain ages (Fig. 5C) an important Mesoproterozoic age cluster with an important statistical peak at 1072 Ma ($n = 13$) and a minor peak at 1493 Ma (Fig. 5). Older single grain ages (Fig. 5C) span from Early Mesoproterozoic to Meso Archean (1493 Ma, 1858 Ma, 2531, 2662 and 2693 Ma) similar to the age distribution pattern observed in sample D7 from the El Tránsito Metamorphic Complex. Concerning the Th/U ratio, as in other two samples, from the 92 zircon analyzed, 41 of them have values ≥0.5 (44.57%), being this ratio in the interval between 2.511 and 0.012 (Table 1, Fig. 4), similar to the obtained figures from sample D7.

5. Discussion

5.1. Maximum depositional age

The youngest zircon grain found in El Tránsito Metamorphic Complex (sample D7), indicates a maximum Late Devonian (380 Ma) depositional age that is coherent with regional geological and geochronological constraints including a new U/Pb age of 282.7 ± 5.8 Ma for a rhyolitic volcanic sequence that overlies the western El Tránsito Metamorphic Complex outcrops (Salazar et al., 2009, see Fig. 1) and the eastern intrusive contact with coarse-grained tonalites (Guanta Unit) of the Elqui-Limarí Batholith (hornblende K/Ar age of 310 ± 8 Ma, Ribba et al., 1988; conventional zircon U/Pb age of 285.6 ± 1.5 Ma, Pankhurst et al., 1996). These ages for the younger zircons are also consistent with the. Rb/Sr "errorchrons" reported previously by Ribba et al. (1988) that were interpreted as resulting from a Carboniferous event of regional metamorphism. Our data are, however, notably different from the detrital zircon age spectra reported by Bahlburg et al. (2009) for a "mica schist of the El Tránsito Metamorphic Complex" (Sample CON90-10), which is characterized by a prominent age maximum between 359 and 250 Ma with the youngest age at 254 ± 7 Ma. Certainly, these ages appear incompatible with the known regional geological relations of the El Tránsito Metamorphic Complex, because there is an U/Pb zircon age at 282.7 ± 5.8 Ma (Salazar et al.,

Table 2
LA-ICP-MS U–Pb zircon data for samples from the Huasco Metamorphic Complex (HMC).

Sample	Concentration			Isotope ratios				Apparent ages (Ma)			
	U (ppm)	Th (ppm)	Th/U	$\frac{^{207}Pb}{^{206}Pb}$	± (%, 1σ)	$\frac{^{238}Pb}{^{206}U}$	± (%, 1σ)	$\frac{^{206}Pb}{^{238}U}$	± (1σ, Ma)	$\frac{^{207}Pb}{^{206}Pb}$	± (1σ, Ma)
HMC: Sample JA8											
JA8_1	212	41	0.2	0.0602	0.0106	10.6965	0.0214	576.1	11.8	612.2	22.7
JA08_8_2	231	79	0.3	0.0823	0.0073	5.3450	0.0205	1105.6	20.8	1252.2	14.2
JA08_8_3	527	75	0.1	0.0862	0.0067	4.3720	0.0199	1327.8	23.8	1342.8	12.8
JA08_8_4	742	359	0.5	0.0618	0.0077	11.0363	0.0201	559.1	10.8	667.0	16.4
JA08_8_5	196	97	0.5	0.0565	0.0108	11.8772	0.0233	521.1	11.7	470.8	23.6
JA08_8_6	942	1174	1.2	0.0582	0.0074	11.5301	0.0207	536.2	10.6	538.2	16.1
JA08_8_7	286	86	0.3	0.0845	0.0098	4.8847	0.0390	1200.6	42.6	1304.2	18.9
JA08_8	1872	1133	0.6	0.0696	0.0065	6.4927	0.0204	923.4	17.6	915.2	13.4
JA08_9	1025	127	0.1	0.0571	0.0070	13.5432	0.0195	459.2	8.6	495.4	15.4
JA08_10	424	203	0.5	0.0921	0.0069	4.1283	0.0216	1398.3	27.2	1469.0	13.1
JA08_11	509	284	0.6	0.0566	0.0085	12.9269	0.0213	480.3	9.9	476.0	18.7
JA08_12	853	408	0.5	0.0588	0.0076	13.3927	0.0213	464.2	9.5	560.5	16.5
JA08_13	253	87	0.3	0.1222	0.0069	2.8177	0.0198	1958.0	33.4	1988.2	12.2
JA08_13	253	87	0.3	0.1222	0.0069	2.8177	0.0198	1958.0	33.4	1988.2	12.2
JA08_13A	226	90	0.4	0.1198	0.0083	3.4952	0.0219	1622.1	31.3	1953.1	14.7
JA08_15	300	377	1.3	0.0900	0.0082	4.2790	0.0415	1353.9	50.5	1425.6	15.6
JA08_16	672	189	0.3	0.0763	0.0073	6.5278	0.0238	918.8	20.3	1102.5	14.6
JA08_17	312	126	0.4	0.0597	0.0091	10.4676	0.0205	588.2	11.5	593.6	19.6
JA08_18	496	252	0.5	0.0582	0.0085	11.4799	0.0216	538.4	11.1	535.9	18.5
JA08_19	416	391	0.9	0.0609	0.0082	10.5697	0.0185	582.7	10.3	635.0	17.6
JA08_20	214	73	0.3	0.0728	0.0085	5.8126	0.0200	1023.3	18.9	1008.3	17.2
JA08_21	121	47	0.4	0.0766	0.0088	5.3461	0.0200	1105.4	20.3	1110.4	17.4
JA08_22	431	290	0.7	0.0596	0.0093	10.8275	0.0234	569.5	12.7	588.0	20.1
JA08_23	941	397	0.4	0.1074	0.0090	3.1613	0.0243	1771.7	37.5	1755.4	16.5
JA08_25	1035	136	0.1	0.0737	0.0087	6.1824	0.0294	966.5	26.3	1034.0	17.5
JA08_26	717	80	0.1	0.1018	0.0070	3.5300	0.0194	1607.9	27.5	1657.2	13.0
JA08_27	1064	591	0.6	0.0600	0.0078	10.3065	0.0191	597.0	10.9	604.8	16.9
JA08_28	717	118	0.2	0.0708	0.0076	6.3932	0.0203	936.8	17.7	952.1	15.5
JA08_29	707	245	0.3	0.0571	0.0089	11.6846	0.0199	529.4	10.1	493.7	19.5
JA08_30	4456	3907	0.9	0.0487	0.0108	84.3527	0.0236	76.0	1.8	133.8	25.3
JA08_31	1546	159	0.1	0.0585	0.0088	10.9145	0.0208	565.1	11.3	550.0	19.2
JA08_32	311	397	1.3	0.0616	0.0098	9.2718	0.0244	660.3	15.3	661.6	21.0
JA08_33	505	161	0.3	0.0894	0.0081	4.1498	0.0207	1391.8	25.9	1413.0	15.4
JA08_34	952	813	0.9	0.0613	0.0084	9.3888	0.0206	652.4	12.7	648.4	17.9
JA08_35	742	314	0.4	0.0802	0.0079	4.8626	0.0211	1205.6	23.1	1201.4	15.5
JA08_36	776	241	0.3	0.0781	0.0081	5.0930	0.0215	1155.7	22.7	1148.2	16.0
JA08_37	363	185	0.5	0.0758	0.0084	5.4664	0.0209	1083.0	20.8	1088.9	16.7
JA08_38	294	89	0.3	0.0743	0.0089	5.8799	0.0213	1012.5	19.9	1049.8	17.9
JA08_39	756	287	0.4	0.0773	0.0080	5.5382	0.0217	1070.1	21.4	1130.1	15.8
JA08_40	1931	205	0.1	0.0873	0.0106	7.2303	0.0267	835.1	20.9	1367.9	20.3
JA08_41	958	286	0.3	0.0627	0.0081	9.4184	0.0196	650.5	12.1	696.5	17.1
JA08_42	2106	1000	0.5	0.0570	0.0082	12.7669	0.0219	486.1	10.2	491.1	18.0
JA08_43	314	102	0.3	0.0909	0.0084	3.9007	0.0217	1471.2	28.4	1443.6	15.8
JA08_44	350	109	0.3	0.0742	0.0084	5.6892	0.0218	1043.8	21.0	1047.4	16.8
JA08_45	1081	473	0.4	0.0570	0.0082	12.7799	0.0201	485.7	9.4	492.3	18.0
JA08_46	1516	1954	1.3	0.0575	0.0109	13.2222	0.0199	470.0	9.0	510.0	23.8
JA08_47	313	106	0.3	0.0746	0.0112	5.6119	0.0214	1057.1	20.8	1058.9	22.3
JA08_48	220	133	0.6	0.0534	0.0144	18.8158	0.0210	333.8	6.8	344.0	32.4
JA08_48A	211	125	0.6	0.0530	0.0147	18.4934	0.0222	339.5	7.3	328.5	32.9
JA08_49	832	67	0.1	0.0571	0.0110	12.6380	0.0205	490.9	9.7	495.6	24.1
JA08_50	87	42	0.5	0.0757	0.0126	5.5819	0.0223	1062.3	21.8	1088.3	25.0
JA08_51	145	106	0.7	0.0854	0.0122	4.3412	0.0226	1336.3	27.2	1323.9	23.4
JA08_52	426	181	0.4	0.0714	0.0112	6.2106	0.0249	962.4	22.3	969.9	22.7
JA08_53	839	121	0.1	0.0831	0.0108	5.0497	0.0222	1164.7	23.6	1271.6	21.0
JA08_54	461	197	0.4	0.0838	0.0108	4.8704	0.0204	1203.9	22.4	1288.7	20.8
JA08_55	176	71	0.4	0.0751	0.0115	5.7920	0.0195	1026.7	18.4	1070.0	22.8
JA08_56	486	70	0.1	0.0573	0.0114	13.1227	0.0205	473.4	9.4	504.1	24.9
JA08_57	384	75	0.2	0.0758	0.0108	5.4696	0.0201	1082.4	20.0	1089.6	21.6
JA08_58	250	203	0.8	0.0945	0.0130	3.5762	0.0268	1589.5	37.7	1518.3	24.2
JA08_59	556	330	0.6	0.0585	0.0114	11.4144	0.0201	541.4	10.4	549.5	24.8
JA08_60	916	761	0.8	0.0581	0.0118	10.6851	0.0225	576.7	12.4	534.8	25.6
JA08_61	305	210	0.7	0.0578	0.0100	11.9133	0.0192	519.6	9.6	524.0	21.8
JA08_62	161	187	1.2	0.0707	0.0109	5.9952	0.0177	994.5	16.3	949.3	22.2
JA08_63	418	162	0.4	0.0783	0.0091	4.9966	0.0179	1176.0	19.2	1153.8	17.9
JA08_64	303	214	0.7	0.0566	0.0112	12.9968	0.0191	477.8	8.8	477.6	24.6
JA08_65	478	550	1.2	0.0537	0.0105	18.1092	0.0194	346.5	6.5	359.5	23.5
JA08_66	468	705	1.5	0.0703	0.0092	8.2731	0.0215	735.6	14.9	937.0	18.7
JA08_67	708	404	0.6	0.0588	0.0095	11.2552	0.0192	548.7	10.1	561.5	20.6
JA08_68	349	214	0.6	0.0865	0.0106	4.2136	0.0216	1372.8	26.6	1350.0	20.4
JA08_69	402	79	0.2	0.0651	0.0097	8.6869	0.0247	702.4	16.4	778.1	20.3
JA08_70	456	115	0.3	0.0787	0.0094	4.8848	0.0207	1200.6	22.6	1165.3	18.5

Table 2 (continued)

Sample	Concentration			Isotope ratios				Apparent ages (Ma)			
	U (ppm)	Th (ppm)	Th/U	$\frac{^{207}Pb}{^{206}Pb}$	± (%, 1σ)	$\frac{^{238}Pb}{^{206}U}$	± (%, 1σ)	$\frac{^{206}Pb}{^{238}U}$	± (1σ, Ma)	$\frac{^{207}Pb}{^{206}Pb}$	± (1σ, Ma)
JA08_71	677	107	0.2	0.0567	0.0094	12.7335	0.0196	487.4	9.2	481.5	20.5
JA08_72	700	375	0.5	0.0569	0.0097	12.7442	0.0199	487.0	9.3	489.4	21.3
JA08_73	685	109	0.2	0.0580	0.0111	12.9574	0.0201	479.2	9.3	531.6	24.1
JA08_74	643	701	1.1	0.1036	0.0087	3.3887	0.0265	1667.0	38.8	1688.8	15.9
JA08_75	228	154	0.7	0.0765	0.0098	5.6755	0.0207	1046.2	20.0	1107.0	19.5
JA08_76	2978	598	0.2	0.0816	0.0095	8.0290	0.0260	756.7	18.6	1236.7	18.6
JA08_77	534	131	0.2	0.0571	0.0105	11.4349	0.0229	540.4	11.8	497.2	23.1
JA08_78	564	184	0.3	0.0568	0.0091	12.5623	0.0191	493.8	9.1	483.0	20.0
JA08_79	377	249	0.7	0.0482	0.0159	51.7305	0.0215	123.4	2.6	111.3	37.2
JA08_80	655	77	0.1	0.0573	0.0089	12.4216	0.0191	499.1	9.2	501.5	19.5
JA08_81	275	50	0.2	0.0622	0.0127	12.8650	0.0279	482.6	13.0	680.6	26.9
JA08_82	153	72	0.5	0.0654	0.0114	7.7438	0.0225	782.9	16.6	788.1	23.7
JA08_83	555	64	0.1	0.0575	0.0094	11.7038	0.0191	528.5	9.7	509.6	20.6
JA08_84	928	565	0.6	0.0770	0.0078	5.5217	0.0193	1073.0	19.1	1120.9	15.5
JA08_85	854	402	0.5	0.0743	0.0081	5.5515	0.0198	1067.7	19.5	1050.6	16.2
JA08_86	188	80	0.4	0.0686	0.0100	6.8338	0.0198	880.4	16.3	885.3	20.5
JA08_87	1035	526	0.5	0.0574	0.0083	11.1164	0.0212	555.3	11.3	507.2	18.1
JA08_88	775	120	0.2	0.1030	0.0081	3.4358	0.0203	1646.8	29.5	1678.5	14.9
JA08_89	513	292	0.6	0.0609	0.0087	10.0886	0.0192	609.3	11.1	634.0	18.7
JA08_90	1202	723	0.6	0.0595	0.0083	10.7772	0.0202	572.0	11.1	585.3	17.9

2009) in Permian acid volcanic rocks that cover in erosive unconformity at El Tránsito Metamorphic Complex (Fig. 2) showing that the assignment of this particular sample needs to be re-assessed.

The maximum depositional age for the Huasco Metamorphic Complex and Choapa Metamorphic Complex is younger than in the El Tránsito Metamorphic Complex, as shown by zircon age peaks at 342 Ma in sample JA08 of Huasco Metamorphic Complex, and 369 and 340 Ma sample LC039 of Choapa Metamorphic Complex (Fig. 5). Slightly younger zircons were reported by Willner et al. (2008) for another sample (06CH54) of the Choapa Metamorphic Complex collected at Playa La Cebada (Fig. 1), which shows a group of zircons with ages ranging from 346 to 299 Ma (peaks weighted means at 333 ± 3 Ma and 304 ± 7 Ma). Also, data for the youngest detrital zircon (294 ± 15 Ma) for a metasandstone sample from the Huasco Metamorphic Complex ("Huasco Beds") reported by Bahlburg et al. (2009) points out to an early Permian maximum depositional age. In any case, these younger ages found in zircons from the coastal metamorphic complexes are consistent with the hypothesis that the El Tránsito Metamorphic Complex may be the internal (eastern) part of an accretionary prism that grew progressively westward during the Carboniferous–Early Permian along the Pacific margin of Western Gondwana.

5.2. Zircon provenance

5.2.1. Sources for Archean to Neoproterozoic zircons

Meso- to Neoarchean zircons such as the 3.0–2.5 Ga ages found in El Tránsito Metamorphic Complex and Choapa Metamorphic Complex samples (Fig. 5) were also identified by Willner et al. (2008) in Choapa Metamorphic Complex sample 06CH54 collected at Playa La Cebada (Fig. 1) and in another sample from the Arrayán Formation, both of which show prominent zircon peaks between 3.4 Ga and 2.6 Ga. Similar old zircons are also present in a sample form the Huasco Metamorphic Complex ("Huasco Beds") analyzed by Bahlburg et al. (2009), who report single grains dated at 3.2 Ga and 2.5 Ga. The source of these old zircons is difficult to trace into well-identified igneous provinces in South America. Willner et al. (2008) although recognizing the problem of the Archean zircon sources suggest they could have derived from multiple recycling from older cratons within Western Gondwana such as the Amazonian, São Francisco, Congo or Río de la Plata

cratons. Yet, the only well-dated magmatic rocks of this age are found as small outcrops at the core of the Nico Pérez terrane in the Río de la Plata craton, near the Atlantic coast of Uruguay (Hartmann et al., 2001; Rapela et al., 2007).

In contrast, possible sources, including magmatic rocks such as those found in the Río de la Plata or Amazonian cratons (Central Amazonian Province, Cordani et al., 2000; Rapela et al., 2007) were certainly available to provide Paleoproterozoic (2.5–2.2 Ga) detrital zircons to the El Tránsito Metamorphic Complex, Choapa Metamorphic Complex and the Huasco Metamorphic Complex sample studied by Bahlburg et al. (2009). Likewise, the sources of the younger group (2.0–1.8 Ga) of Paleoproterozoic zircons may be traced into the Trans Amazonian Mobile Belt of northern and Central Brazil (Ventuari-Tapajos Province, Cordani et al., 2000; Chew et al., 2008; Bahlburg et al., 2009; Tohver et al., 2010).

Mesoproterozoic zircons such those found in the El Tránsito, Huasco and Choapa metamorphic complexes are of common occurrence in diverse geological provinces of western Gondwana, including the Sunsas–Grenville Belt along the western edge of the Amazon craton in Bolivia and Brazil (Chew et al., 2008; Cordani et al., 2010; Ramos, 2010), the Arequipa–Antofalla block (Wörner et al., 2000; Loewy et al., 2004), the Sierra de Maz, Sierra Pie de Palo in western Sierras Pampeanas (McDonough et al., 1993; Vujovich et al., 2004; Casquet et al., 2008) and the basement to the early Paleozoic Precordillera carbonate platform (Kay et al., 1996; Rapela et al., 2010; Thomas et al., 2004). Moreover, Mesoproterozoic zircon ages are a common feature in most of the early Paleozoic sedimentary sequences of central western Argentina (i.e. Escayola et al., 2007; Collo et al., 2009; Ramos, 2010) and do not represent a discriminant factor in order to interpret sources.

As previously described, an important proportion of the analyzed zircons have Th/U ratios ≥0.5 (Tables 1 and 2) that could be interpreted, according to Hoskin and Schaltegger (2003) as indicative of an igneous origin. In this sense, Neoproterozoic magmatic rocks (700–550 Ma), which may supply detrital zircons for the El Tránsito Metamorphic Complex, Huasco Metamorphic Complex and Choapa Metamorphic Complex samples analyzed in this work, occur in southeastern Brazil and near the Atlantic coast of Argentina, in regions that were affected by the Brasiliano–Pan African Orogeny attributed to the collision of the Amazonian and Sao Francisco cratons and the assembly of Western Gondwana (Rapela et al, 2010;
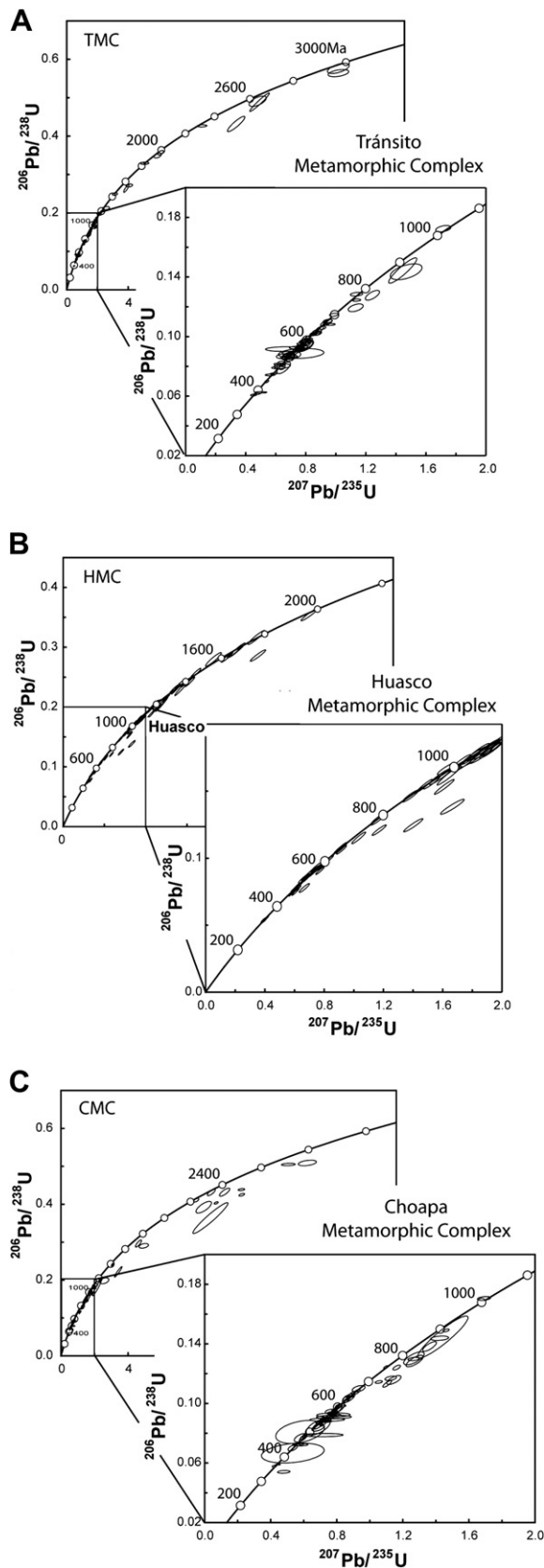
Fig. 3. Concordia diagrams of LA-ICP-MS zircon from: (A) the El Tránsito Metamorphic Complex (sample D7); (B) Huasco Metamorphic Complex (sample JA08); and (C) Choapa Metamorphic Complex (sample LC03). Enlargements show data distribution within ages <1 Ga.

Tohver et al., 2010). Neoproterozoic intrusives (635 ± 5 Ma) have been reported also in the Arequipa–Antofalla block in a dacitic dike in Quebrada Choja at northern Chile (Loewy et al., 2004). Although outcrops of these rocks may be too far to be considered as a sedimentary source for the El Tránsito Metamorphic Complex and Choapa Metamorphic Complex, 0.7–0.6 Ga detrital zircons have been recorded in low-grade early Paleozoic metamorphic rocks of the Puncoviscana formation (Adams et al., 2008), the eastern Sierras Pampeanas (Escayola et al., 2007), and, further to the west at Sierra de Famatina (Collo et al., 2009, see below).

Despite the unresolved source problem for the older group of Archean zircons (3.2–2.5 Ga), the Proterozoic zircons found in the El Tránsito Metamorphic Complex and Choapa Metamorphic Complex can be derived from recycling of any of the geological provinces and domains mentioned above: The Amazonian (Central Amazonian and Ventuari-Tapajos Provinces) or the Río de la Plata cratons for the Paleoproterozoic zircons, the Grenville–Sunsas belt or the Cuyania basement for the Mesoproterozoic zircons, and the Brasiliano–Pan African Orogenic Belts for the Neoproterozoic group. However, as these detrital zircons were, possibly, incorporated into accretionary complexes along the Paleo-Pacific margin after the Devonian, they do not provide independent information allowing to discriminate the existence or not of Chilenia. Thus, they do not test the hypothesis of Chilenia being an independent crustal block with a distinct geological history.

5.2.2. Late Neoproterozoic to early Cambrian (575–535 Ma) Zircons. A Chilenia source?

The largest zircon population in the El Tránsito Metamorphic Complex and Choapa Metamorphic Complex corresponds, by far, to the late Neoproterozoic–earliest Cambrian assemblage (peaks at 569 Ma and 535 Ma in sample D7; and 568 Ma and 545 Ma in LC03). Zircons of this age also form the second largest subpopulation in the Huasco Metamorphic Complex (peaks at 575 and 540 Ma in sample JA08, Fig. 5B). The same group is also well represented in sample 06CH54 form the Choapa Metamorphic Complex (547 Ma, $n = 7$, Willner et al., 2008). Zircons in this age range also occur in the Filo Gris Complex, considered by Astini and Cawood (2009) as a part of the pre-collisional sedimentary cover of Chilenia. The detrital zircon spectra of Filo Gris sample SA30 shows a major Mesoproterozoic (1.02–1.45 Ga) group along with minor groupings at 613 Ma ("Brasiliano" ages) and 548 Ma ($n = 2$); this last comparable with the dominant age cluster of the Chilean accretionary complexes. Zircons of the same age have been found in the Devonian accretionary HP/LT Guarguaraz Complex, (sample 06CH18 of Willner et al., 2008), that includes a broad age cluster at 0.94–1.45 Ga (95% of the population) but also contains younger concordant zircons dated at 555 ± 8 and 581 ± 8 Ma that represent a possible magmatic event at the end of the Neoproterozoic. Altogether, these data show that a significant late Neoproterozoic zircon population (570–530 Ma) appears intimately related to the inferred Chilenia terrane, either in units interpreted as pre-collisional (like the Filo Gris Complex), syncollisional (like the Guarguaraz Complex in the eastern accretionary prism) or post docking (like those in the El Tránsito, Choapa and Huasco etamorphic complexes as parts of the western subduction complexes). The precise determination of provenance for this group is not easy because no pervasive igneous event has yet been discovered in the exotic terranes previously amalgamated to Gondwana (i.e. Precordillera or Cuyania), the Western Sierras Pampeanas, or in the Famatina belt that should have been the most likely sources to provide Neoproterozoic zircons, at least to the post-docking Chilean accretionary complexes.

The only known intrusive of this age in the Western Sierras Pampeanas corresponds to small outcrops of a 570 Ma
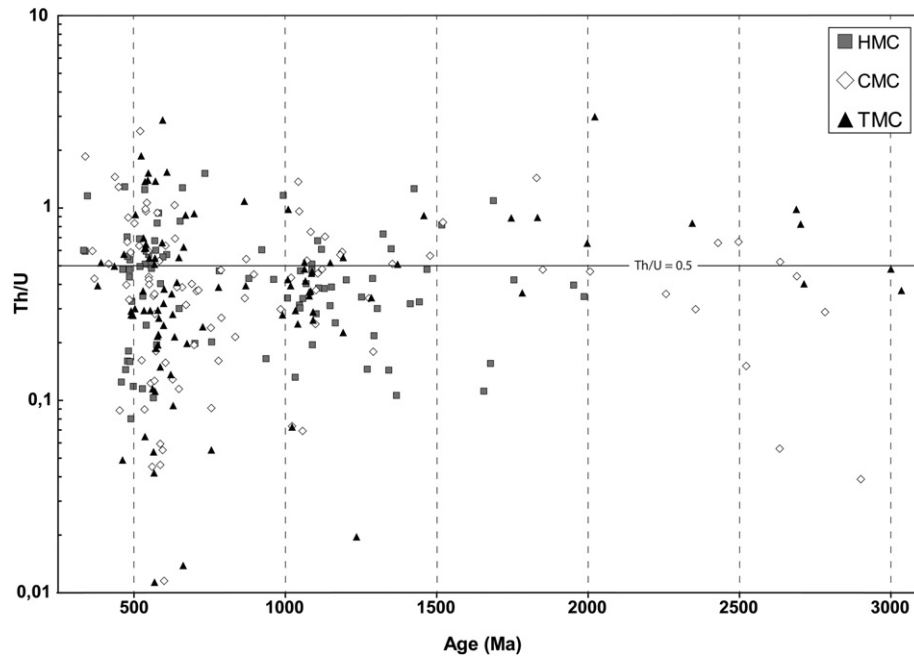
Fig. 4. Th/U versus age of zircons from the Huasco, Choapa and El Tránsito metamorphic complexes. The horizontal black line (Th/U = 0.5) represents the limit between igneous and metamorphic zircons (Hoskin and Schaltegger, 2003).

syenite−carbonatite complex intruding the Grenville age basement of Sierra de Maz at 29°15′S (Casquet et al., 2008). A recycling origin for this such important population is also difficult to invoke, because no significant Late Proterozoic−Early Cambrian zircon populations has been identified in the early Paleozoic sedimentary sequences that outcrop at Sierra de Famatina or the Precordillera. Only a few zircons of this age have been found in the sediments of the late Neoproterozoic−Early Cambrian Caucete Group (Borrello, 1969) exposed at Sierra de Pie de Palo (San Juan) which apparently contains the sedimentary record of rifting and early drift of the Precordillera from Laurentia (Vujovich et al., 2004; Naipauer et al., 2010). The lower units within the Caucete Group include, besides a large population of Mesoproterozoic zircons derived from a Grenvillian sources, a minor group of magmatic zircons with ages between 570 Ma and 530 Ma, considered by Naipauer et al. (2010) as recording magmatism associated to the breakup and separation of the Precordillera and Laurentia. Nevertheless, this signal disappears up-section in the Lower Cambrian, drift-stage Angaco Formation, exclusively dominated by Grenville or older zircon populations. This is also true from the Lower Cambrian Cerro Totora Formation within the sedimentary cover of the Precordillera that is a possible equivalent at the base of the passive margin succession and includes detrital zircons in the age range from 1890 to 970 Ma compatible with typical sediment supply from different Laurentian basement provinces (Thomas et al., 2004). Worth is to note, that the only quartz-rich sandstone interval within the Early Cambrian carbonate drift succession in the La Laja Formation yielded, apart from a large Grenville main peak, a single zircon grain of 535 ± 9 Ma (Astini et al., 2005) indicating that at least few ages compatible with the 539−530 Ma synrift igneous rocks (rhyolites and granites) derived from the Southern Oklahoma-Wichita rift system were being recycled.

Detrital latest Neoproterozoic−Early Cambrian zircons are also uncommon in the early Paleozoic low-grade sedimentary units (Negro Peinado and Achavil formations) cropping out further east, at Sierra de Famatina, ∼350 km due east of the outcrops of El Tránsito Metamorphic Complex. These two units, considered by Collo et al. (2009) as synorogenic deposits of the Early Cambrian Pampean Cycle, include Paleoproterozoic to Cambrian zircon populations, which are consistent with their derivation from eastward Gondwana sources, showing only a few zircons with ages between the Pampean and Brasiliano peaks, 641 ± 25 and 522 ± 8 Ma in the Negro Peinado Formation, 632 ± 13 and 519 ± 23 Ma in the Achavil Formation (Collo et al., 2009).

Intrusives and metasedimentary sequences that can, hypothetically may have provided detrital zircons for the Chilean metamorphic complexes can be found only at larger distances, at Sierra Norte de Córdoba (easternmost Sierras Pampeanas) where some rhyolitic ignimbrites interbedded in metaconglomerates of La Lidia Formation were dated by Llambías et al. (2003) at 584 Ma (U/Pb). This value slightly older than the oldest peaks that we have found in the late Proterozoic−Early Cambrian groups in the El Tránsito Metamorphic Complex (569 Ma), Huasco Metamorphic Complex (575 Ma) and Choapa Metamorphic Complex (568 Ma) although a large and younger calc-alkaline batholith that outcrop in Sierra Norte and extends discontinuously southward along the easternmost margin of Sierras de Córdoba have yield numerous younger U/Pb ages between ca. 555 and 525 Ma (Schwartz et al., 2008; Ramos et al., in press; Siegesmund et al., 2010). Also a detrital zircon population with ages ranging from 590−550 Ma has been found further to the south in Sierra de San Luis (metasediments of the San Luis Formation, Conlara Metamorphic Complex, Drobe et al., 2009; Siegesmund et al., 2010), However, with the exception of the Sierra de San Luis, detrital Neoproterozoic zircons are not of common occurrence in high grade late Neoproterozoic−Cambrian metasedimentary units (>530 Ma) of the eastern Sierras Pampeanas, as it is the case in Sierras de Córdoba, where Schwartz and Gromet (2004) have found Neoproterozoic (600−700 Ma), Mesoproterozoic (950−1050 Ma) and Paleoproterozoic (>1900 Ma) detrital zircons, but no traces of zircons in the 570−530 Ma age range.

Other geological units that can be referred as a potential source for latest Proterozoic−Early Cambrian zircons include the low-grade metaturbidites of the Puncoviscana Formation, with extensive outcrops along the Eastern Cordillera of Salta and Jujuy (Aceñolaza and Aceñolaza, 2007; Ramos, 2009; Adams et al., 2010). This formation, probably equivalent to the high grade rocks of the eastern
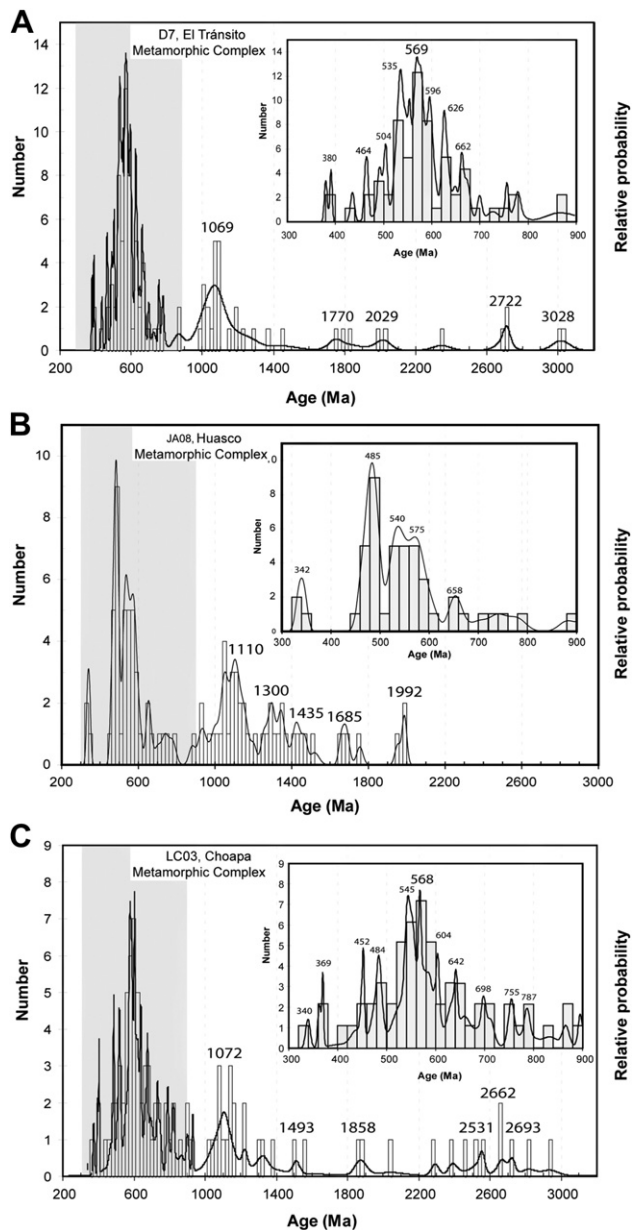
Fig. 5. Zircon probability density plots from: (A) the El Tránsito Metamorphic Complex (sample D7); (B) Huasco Metamorphic Complex (sample JA08); and (C) Choapa Metamorphic Complex (sample LC03). Enlargements show zircons with ages <1 Ga.

Sierras Pampeanas (see Ramos et al., in press and references therein) is uncomformably covered by Upper Cambrian quartz-rich sedimentary rocks of the Mesón Group (Aceñolaza and Aceñolaza, 2007; Astini, 2008). The Puncoviscana Formation generally includes distinct zircon subpopulations of Neoproterozoic (1150–850 Ma) and Brasiliano (650–600 Ma) ages and a younger group with ages between 530 and 514 Ma (Adams et al., 2010). Some samples, apparently collected form the upper levels of the formation; contain 580–530 Ma zircons that have also been found in the overlying Mesón Group (Adams et al., 2008; Hauser et al., in press). While the sources for the last group are unknown, 530–510 Ma zircons may be linked, somehow, to local volcanic sources (Coira et al., 1990) and/or to granitod stocks emplaced in the Puncoviscana basin during the Early Cambrian (i.e. Tastil, Cañani, Tipayoc, Chañi plutons; 534–517 Ma) (Aceñolaza and Aceñolaza, 2007; Ramos, 2008; Hongn et al., 2010; Hauser et al., in press).

This survey through the literature show that some potential distant sources for Proterozoic–Early Cambrian detrital zircons exist in the easternmost Sierras Pampeanas and/or the Puncoviscana basin. Nevertheless, similar potential sources are virtually absent in terranes surrounding Chilenia (Precordillera/Cuyania and Western Sierras Pampeanas), which should have acted as the main sources of sediments along the western Gondwana margin during and after accretion of Chilenia. This makes difficult to explain how the remarkable population of late Neoproterozoic–Early Cambrian zircons in our samples got to the western subduction complexes. As a possible solution we suggest they were derived from the erosion of primary magmatic sources within Chilenia itself. Such sources should have also provided sediments to a pre-collisional sedimentary cover (i.e. Filo Gris Complex) to the eastern accretionary prism (Guarguaraz Complex), when Chilenia was approaching and colliding with Gondwana, as well as to the western flank of the terrane, in Chile, where post-collisional accretionary complexes developed by the Carboniferous.

A similar question about the origin of latest Neoproterozoic–Early Cambrian detrital zircon populations in metamorphic and sedimentary formations from the eastern Cordillera of Ecuador and Perú (Marañón Complex and others) has been recently raised by Chew et al. (2008), Cardona et al. (2009) and Reimann et al. (in press). These units contain a major group of zircons with an age range between 555 and 520 Ma. Although other detrital zircon groups found in these units could be derived form recycling of the Arequipa Massif or from magmatic belts along the Paleozoic margin of Gondwana, Chew et al. (2008) pointed out that no potential sources for this group of zircons are known form the northern and central Andes. Derivation from eastern Amazonia was considered unlikely due to the lack of detritus derived from the core of the Amazonian craton in the Paleozoic sedimentary sequences of the Eastern Cordillera (see also Cardona et al., 2009). As a solution, these authors and later Reimann et al. (in press) proposed a source linked to an "unknown late Neoproterozoic magmatic belt" buried beneath the present-day Andean belt or under the Amazon Basin. Cardona et al. (2009) also considered that the major feeder of the extensive Neoproterozoic to Cambrian zircon found in the Marañón schist belts must be related to a major felsic-intermediate magmatic source that is more likely to have a continental arc affinity.

This suggestion may have implications for the history of breakup of Rodinia and specifically opening of Iapetus (a paleo-Pacific Ocean) and initiation of paleo-Pacific crust subduction. Cawood (2005) suggested that initiation of subduction and initial assembly and collision of rifted/detached blocks to Gondwana along the Terra Australis Orogen occurred at different times in East (580–570 Ma) and West Gondwana (530 Ma). The presence of a late Proterozoic magmatic arc in the Central Andes of Perú gives support to Cardona et al. (2009) suggestion of an earlier separation between Amazonia and Baltica-Laurentia followed by inception of an active margin operated by subduction along the western Gondwana margin since at least 640 Ma. Yet, it is worth to mention that the hypothetical magmatic arc has not been traced to the south into the Chilenia terrane, given that the interposed Arequipa–Antofalla block has no magmatic rocks or sedimentary sequences carrying late Neoproterozoic–early Cambrian zircons (see Wasteneys et al., 1995; Wörner et al., 2000; Loewy et al., 2004; Chew et al., 2008; Casquet et al., 2010; Riemann et al., in press).

Our study on the metasedimentary assemblages to both sides of the inferred Chilenia terrane would provide strong indirect evidence to the existence of an authocthonous subduction-related late Neoproterozoic–Early Cambrian igneous source within the basement of Chilenia. The location of the Chilenia terrane in relation to western Gondwana or the Arequipa Massif during the late Proterozoic is unknown, but it may have been early detached from

Laurentia (Keppie and Ramos, 1999) before being transferred to its present position.

5.2.3. Paleozoic (530–342 Ma) zircons: Gondwana sources

Within the younger zircons found in the El Tránsito Metamorphic Complex, the middle Cambrian (504 Ma) zircons of sample D7 were, perhaps, derived from the erosion of igneous rocks emplaced in the Eastern Cordillera (I-type intrusives in the Puncoviscana Basin) and/or the Sierras Pampeanas during the Pampean Orogeny (Rapela et al., 1998; Ramos, 2009; Schwartz et al., 2008; Ramos et al., in press; Siegesmund et al., 2010). The younger and numerous Ordovician (480–450 Ma) zircons that appear in the El Tránsito Metamorphic Complex (peak at 464 Ma) and form the largest fraction of the detrital zircon population in Huasco Metamorphic Complex (peak at 485 Ma), also stands out clearly in sample HU4, from Huasco Metamorphic Complex (Bahlburg et al., 2009). Ordovician zircons such as those found in the Choapa Metamorphic Complex (peaks at 484 and 452 Ma) were also found by Willner et al. (2008) not only in the Choapa Metamorphic Complex, but also in the Arrayán Formation. Worth is to note that, in contrast to the Chilean accretionary complexes, Ordovician zircons younger than 556 Ma have not been found in the Guarguaraz Complex (Willner et al., 2008) or in the Filo Gris Complex (Astini and Cawood, 2009), where Ordovician zircons are totally absent, even if they are very numerous or dominate within the detrital populations in the surrounding Late Paleozoic sedimentary formations of western Argentina. The lack of any Ordovician to Early Devonian detritus in these pre-collisional units of Chilenia affinities seems to indicate not only that during the early Paleozoic a barrier prevented sources from the Gondwana margin, but also reveals the absence of early Paleozoic arcs in the Chilenia microplate (see below). It was only after the docking of Chilenia that sediments derived from the erosion of the large Ordovician Famatinian arc (Coira et al., 1999; Astini and Dávila, 2004; Astini et al., 2007; Collo et al., 2009; Ramos, 2009), were able to by-pass Chilenia and reach the western, post-collisional accretionary prism.

Late Devonian–Mississippian zircons form the youngest groups in the El Tránsito Metamorphic Complex (380 Ma), Huasco Metamorphic Complex (342 Ma) and Choapa Metamorphic Complex (369 and 340 Ma peaks) (Fig. 5). Although this group is represented only by a few grains in our samples, zircons of this age range form a very prominent peak in samples from the Arrayán Formation (341 Ma) and Choapa Metamorphic Complex (331 Ma) (Willner et al., 2008). Granite pebbles of this age (333 Ma) have also been found in the early Permian Huentelauquén Formation that uncomformably cover the Choapa Metamorphic Complex near Los Vilos (Willner et al., 2008). These detritus are too young to be derived from the Famatinian arc in Argentina and too old to be derived from the erosion of the late Paleozoic magmatic arc (e.g. the Elqui-Limarí Batholith) formed along the Pacific margin of Gondwana after reinitiation of subduction subsequent to the amalgamation of Chilenia (Mpodozis and Kay, 1992). The age of the oldest dated late Paleozoic supra-subduction I-type granitoids known in the Frontal Cordillera do not exceed 320 Ma (Ribba et al., 1988; Pankhurst et al., 1996; Mpodozis and Kay, 1992), which led Willner et al. (2008) infer that the older, late Devonian–Early Carboniferous, zircons reflect an "unknown, relatively proximal magmatic event" associated to partial melting of a late Mesoproterozoic crust.

A possible source for these zircons has been recently found in several localities in western Argentina. Samples from rhyolitic volcanic sequences previously attributed to the Ordovician Las Planchadas Formation at Cazadero Grande, La Rioja ($\sim 28°$ SL) yield a 348 ± 3 Ma U/Pb SHRIMP age (Martina et al., 2007; Martina et al., 2010). Other samples of rhyolites collected further south at Cerros

Pabellones (27°30′S) uncomformably cover the Mesoproterozoic basement of western Sierras Pampeanas and have been dated at 342 ± 1 Ma (Martina and Astini, 2009; Martina et al., 2010). Also a set of detrital ages within a volcano-sedimentary succession at the base of the Carboniferous near Jagüe (27°S), has allowed identification of a large dominant detrital peak at 336 Ma (Martina and Astini, 2009), whereas a recent date on a primary volcanic flow within the same interval yielded 336 ± 0.06 Ma (Gulbranson et al., 2010). Within this same region, in Sierra de Las Minitas, Coughlin (2000) dated several bi-modal dykes intruding folded Early Devonian rocks yielding an age range between 364 and 346 Ma. Plutons largely bracketed between 360 and 325 Ma and similar petrological characteristics intrude the basement of the Sierras Pampeanas further to the east (Dahlquist et al., 2006, 2010; Grosse et al., 2008). Astini et al. (2009) have shown that this magmatic suite includes an important component of bi-modal volcanism with an intraplate signature and juvenile influence resulting from a widespread magmatic episode associated to extensional collapse and crustal melting after the docking of Chilenia at approximately 390 Ma (Davis et al., 1999; Willner et al., 2009b). Erosion of these relatively proximal sources may easily explain the Devonian and early Carboniferous zircon ages within the El Tránsito, Huasco and Choapa metamorphic complexes.

5.3. Open questions: subduction polarity and the "missing" Siluro-Devonian magmatic arc

The process of accretion and docking necessarily implies closure and removal via subduction of the oceanic space that separated the Chilenia microplate from Gondwana, even if the position and polarity of the related subduction zone has remained a controversial topic. Ramos et al. (1984, 1986) and Mpodozis and Ramos (1989) initially suggested an east-dipping subduction in order to explain a structural belt known as the Proto-Precordillera in western Argentina, although later studies have cast some doubts on the existence of such tectonic element (Astini, 1996). The fact that no typical Silurian and Devonian Andean-type magmatic belt has been found so far within the Gondwana margin of western Argentina allowed alternative suggestions showing subduction dipping to the west (Astini et al., 1995; Davis et al., 1999) . A main argument that led Ramos et al. (1984, 1986) to propose an east-dipping subduction is the west-verging folding affecting the early Paleozoic outcrops of the westernmost Precordillera. This transport direction to the west was taken as a strong argument supporting the accretionary prism dynamics related to east-dipping subduction. More recently, Davis et al. (1999) pointed out that the transport direction had been opposite to previous suggestions and obduction of mafic-ultramafic layer complexes within continental margin crust of eastern Chilenia onto the Precordillera Terrane could be better explained by west-dipping subduction.

Zircon provenance analysis may allow an independent test. If metagreywakes at Filo Gris or at Guarguaraz complexes were part of the sedimentary cover or a subduction complex along the eastern Chilenia margin and subduction was to the west then they should include at least a few Silurian–early Devonian zircons. Yet detrital zircons of this age are absent in the samples from these two units that outcrop 550 km apart along the eastern edge of the Frontal Cordillera. This clearly differentiates these rocks from all of the late Paleozoic sedimentary units to the east, invariably yielding Famatinian (largely Ocloyic) and early Carboniferous magmatic zircons (Ezpeleta et al., 2009). The fact that very few ages younger than Neoproterozoic have been recorded within the Guarguaraz and Filo Gris complexes means not only that this terrane was detached from the Gondwana margin, but also that it was most probably the downgoing plate in any possible convergent tectonic

scenario as suggested by Mpodozis and Ramos (1989); Massonne and Calderón (2008) and Willner et al. (2011). Yet the problem remains unsolved as no well-developed Late Ordovician to Early Devonian subduction-related arc rocks have been found along the early Paleozoic Gondwana margin in western Argentina. As an alternative, Astini and Dávila (2005, 2006) suggested the possibility of segmentation and flat subduction within the Central Andean Segment in order to avoid arc magmatism within the upper plate.

6. Conclusions

The age of detrital zircon populations of the El Tránsito, Huasco and Choapa metamorphic complexes is compatible with a model suggesting development of a large accretionary prism along the western margin of Chilenia after its accretion to Gondwana in the Devonian. Buildup of the accretionary prism complex began possibly simultaneously with the beginning of late Paleozoic subduction along the western margin of Gondwana giving rise to the emplacement of the large Frontal Cordillera batholiths after a precollisonal period, during which the western margin of Chilenia may have evolved as a passive continental margin. The fact that the maximum age of sedimentation, indicated by the age of the youngest detrital zircons, is older in the El Tránsito Metamorphic Complex (380 Ma) than in our samples from the Huasco Metamorphic Complex (342 Ma) and Choapa Metamorphic Complex (340 Ma), shows that the accretionary prism grew progressively toward the west during the Carboniferous–early Permian. It is clear from our data set that latest Devonian–Early Carboniferous as well as Ordovician sources derived from the east started bypassing the continental margin toward the Late Carboniferous (Pennsylvanian), after reinitiation of subduction. This implies development of a drainage system directed to the west that may have entrenched and allowed sampling into the Chilenia basement, therefore providing the distinct autochthonous set of Late Proterozoic–Early Cambrian ages shown in our data.

Even if the El Tránsito Metamorphic Complex and Choapa Metamorphic Complex include rare Archean (3.0–2.5 Ga) zircons, older than some of the oldest units of the Amazonian craton, detrital zircon populations in the three complexes include age groups that can be explained by the erosion from sources within Gondwana or peripheral terranes like Famatina or Precordillera. The El Tránsito Metamorphic Complex, Huasco Metamorphic Complex and Choapa Metamorphic Complex include a notable Mesoproterozoic zircon age grouping (1.3–1.0 Ga) which is compatible with its provenance from sources of common occurrence in the basement of the Cuyania terrane, the Arequipa–Antofalla block or the Grenville–Sunsas belt. Zircons with ages between 640 and 600 Ma may derive from sources in the Brasiliano/Pan African Orogenic belt while the 480–450 Ma peak may be explained by the erosion and recycling of the Famatinian magmatic arc. Zircons in the 380–340 Ma age range probably derive from the erosion of recently identified Devonian–early Carboniferous acid volcanic sequences and intrusives formed during the extensional collapse that may have followed the collision of Chilenia.

The origin of the very large Neoproterozoic–Early Cambrian (575–530 Ma) subpopulation of zircons, that dominates the detrital fraction in the El Tránsito Metamorphic Complex and Choapa Metamorphic Complex and forms a large group in the Huasco Metamorphic Complex, cannot be easily explained. Although we cannot completely rule out a distal derivation from a still poorly defined magmatic system located in the eastern Sierras Pampeanas, the absence of zircons of this age, both in Neoproterozoic–Early Cambrian sedimentary sequences in the Sierras Pampeanas and their scarcity in the lower Paleozoic sediments in the Famatina belt, indicates that they are derived from a close igneous source, most probably unrelated to Gondwana. This work allows an independent test to the existence of Chilenia as a microcontinental terrane that was accreted to the central Andean margin during the Devonian.

References

Aceñolaza, G., Aceñolaza, F., 2007. Insights in the Neoproterozoic–early Cambrian transition of NW Argentina: facies, environments and fossils in the proto-margin of Gondwana. In: Geological Society, London, Special Publications, vol. 286 1–13.

Adams, C.J., Miller, H., Toselli, A.J., Griffin, W.L., 2008. The Puncoviscana formation of northwest Argentina: U–Pb geochronology of detrital zircons and Rb–Sr metamorphic ages and their bearing on its stratigraphic age, sediment provenance and tectonic setting. Neues Jahrbuch für Geologie und Paläontologie – Abhandlungen 2 (247/3), 341–352.

Adams, C.J., Miller, H., Aceñolaza, F.G., Toselli, A.J., Griffin, W.L., 2010. The Pacific Gondwana margin in the late Neoproterozoic–early Paleozoic: Detrital zircon U–Pb ages from metasediments in northwest Argentina reveal their maximum age, provenance and tectonic setting, Gondwana Research (available online).

Astini, R.A., 1996. Las fases diastróficas del Paleozoico medio en la Precordillera del oeste argentino: evidencias estratigráficas. In: XIII Congreso Geológico Argentino y III Congreso de Exploración de Hidrocarburos, vol. 5, pp. 509–526. Buenos Aires.

Astini, R., 2008. Sedimentación, facies, discordancias y evolución paleoambiental durante el Cambro-Ordovícico. In: Coira, B., Zapettini, E. (Eds.), XVII Congreso Geológico Argentino, Relatorio, pp. 50–73.

Astini, R., Dávila, F., 2004. Ordovician back arc foreland and Ocloyic thrust belt development on the western Gondwana margin as a response to Precordillera terrane accretion. Tectonics 23, 19. doi:10.1029/2003TC001620. TC4008.

Astini, R.A., Dávila, F.M., 2005. Links and contrasts between Paleozoic orogens along the Central Andes Meeting Gondwana 12, Abstracts: 50. Mendoza.

Astini, R.A., Dávila, F.M., 2006. Paleozoic flat slab subduction and broken foreland scenarios prior to the Andes Mountain building. Backbone of the Americas. Speciality Meeting No. 2. In: Geological Society of America Abstracts with Programs , Mendoza75–76.

Astini, R.A., Cawood, P.A., 2009. A Proterozoic basement under the northern Cordillera Frontal: A hint to Chilenia and the continuation of the accretionary prism east of Precordillera?. In: XII Congreso Geológico Chileno, Abstract S9_012 Santiago4.

Astini, R.A., Benedetto, J.L., Vaccari, N.E., 1995. The early Paleozoic evolution of the Argentine Precordillera as a Laurentian rifted, drifted, and collided terrane A geodynamic model. Geological Society of America Bulletin 107 (3), 253–273.

Astini, R.A., Thomas, W.A., McClelland, W.C., 2005. Provenance of Middle Ordovician detritus in the Argentine Precordillera. Meeting Gondwana 12, Abstracts: 51. Mendoza.

Astini, R.A., Collo, G., Martina, F., 2007. Ordovician K-bentonites in the upperplate active margin of Western Gondwana (Famatina Ranges): stratigraphic and palaeogeographic significance. Gondwana Research 11, 311–325.

Astini, R.A., Martina, F., Ezpeleta, M., Dávila, F., Cawood, P., 2009. Chronology from rifting to foreland basin in the Paganzo Basin (Argentina), and a reapprisal on the "Eo- and Neohercynian" tectonics along Western Gondwana. In: XII Congreso Geológico Chileno, Abstract S9-010 Santiago4.

Bahlburg, H., Vervoort, J.D., Andrew Du Frane, S., Bock, B., Augustsson, C., Reimann, C., 2009. Timing of crust formation and recycling in accretionary orogens: Insights learned from the western margin of South America. Earth-Science Reviews 97, 215–241.

Bell, C.M., 1984. Deformation produced by the subduction of a Paleozoic turbidite sequence in northern Chile. Journal of the Geological Society of London 141, 147–168.

Borrello, A.V., 1969. Los geosinclinales de la Argentina. Dirección Nacional d Geología y Minería, Anales 14, 1–136. Buenos Aires.

Cardona, A., Cordani, U.G., Ruiz, J., Valencia, V.A., Armstrong, R., Chew, D., Nutman, A., Sanchez, A.W., 2009. U–Pb Zircon Geochronology and Nd Isotopic Signatures of the Pre- Mesozoic metamorphic basement of the eastern Peruvian Andes: growth and Provenance of a Late Neoproterozoic to Carboniferous accretionary Orogen on the northwest margin of Gondwana. The Journal of Geology 117, 285–305.

Casquet, C., Pankhurst, R.J., Galindo, C., Rapela, C.W.C., Fanning, M., Baldo, E., Dahlquist, J., González Casado, J.M., Colombo, F., 2008. A deformed alkaline igneous rock–carbonatite complex from the Western Sierras Pampeanas,

Argentina: Evidence for late Neoproterozoic opening of the Clymene Ocean? Precambrian Research 165, 205—220.

Casquet, C., Fanning, C.M., Galindo, C., Pankhurst, R.J., Rapela, C.W., Torres, P., 2010. The Arequipa Massif of Peru: New SHRIMP and isotope constraints on a Paleo-proterozoic inlier in the Grenvillian orogen. Journal of South American Earth Sciences 29, 128—142.

Cawood, P.A., 2005. Terra Australis Orogen: Rodinia breakup and development of the Pacific and Iapetus margins of Gondwana during the Neoproterozoic and Paleozoic. Earth-Science Reviews 69, 249—279.

Chang, Z., Venvoort, J.D., Mccellnad, W.C., Knaack, Ch, 2006. U—Pb dating of zircon by LA-ICP-MS. Geochemistry, Geophysics, Geosystems vol. 7. doi:10.1029/2005GC001100 Q05009.

Chew, D., Magnab, T., Kirkland, C., Miskovic, C., Cardona, A., Spikings, R., Schaltegger, U., 2008. Detrital zircon fingerprint of the Proto-Andes: Evidence for a Neoproterozoic active margin? Precambrian Research 167, 186—200.

Coira, B.L., Manca, N., Chayle, W.E., 1990. Registros volcánicos en la Formación Puncoviscana. In: Aceñolaza, F.G., Miller, H., Toselli, A.J. (Eds.), El Ciclo Pam-peano en el noroeste Argentino, vol. 4. Universidad Nacional de Tucumán, San Miguel de Tucumán, pp. 53—60.

Coira, B.L., Kay, S.M., Pérez, B., Woll, B., Hanning, M., Flores, P., 1999. Magmatic sources and tectonic setting of Gondwana margin Ordovician magmas, northern Puna of Argentina and Chile. In: Ramos, V.A., Keppie, D. (Eds.), Lau-rentia Gondwanan Connections before Pangea. Geological Society of America Special Paper 336, pp. 145—170.

Collo, G., Astini, R.A., Cawood, P., Buchan, C., Pimentel, M., 2009. U—Pb detrital zircon ages and Sm—Nd isotopic features in low-grade metasedimentary rocks of the Famatina belt: implications for late Neoproterozoic—early Palaeozoic evolution of the proto-Andean margin of Gondwana. Journal of the Geological Society, London 166, 303—319.

Cordani, U.G., Milani, E.J., Thomaz Filho, A., Campos, D.A., 2000. Tectonic Evolution of South America. In: 31st International Geological Congress. Brazilian Academy of Sciences Rio de Janeiro, Brazil.

Cordani, U.G., Fraga, L.M., Reis, N., Tassinari, C., Brito-Neves, B., 2010. On the origin and tectonic significance of the intra-plate events of Grenvillian-type age in south America: a discussion. Journal of South American Earth Sciences 29, 143—159.

Corfu, F., Hanchar, J.M., Hoskin, P.W.O., Kinny, P.D., 2003. Atlas of zircon textures. Reviews in Mineralogy and Geochemistry 53, 469—500.

Coughlin, T.J., 2000. Linked Origen-Oblique Fault Zones in the Central Argentine Andes: The Basis for a New Model for Andean Orogenesis and Metallogenesis, Ph. D Thesis, Univerity of Queensland, p. 207.

Dahlquist, J.A., Pankhurst, R.J., Rapela, C.W., Casquet, C., Fanning, C.M., Alasino, P., Báez, M., 2006. The San Blas Pluton: an example of Carboniferous plutonism in the Sierras Pampeanas, Argentina. Journal of South American Earth Sciences 20, 341—350.

Dahlquist, J.A., Alasino, P., Eby, G., Galindo, C., Casquet, C., 2010. Fault controlled Carboniferous A-type magmatism in the proto-Andean foreland (Sierras Pam-peanas, Argentina): Geochemical constraints and petrogénesis. Lithos 115 (1—4), 65—81.

Dahlquist, J.A., Pankhurst, R.J., Rapella, C.W., Galindo, C., Alasino, P., Fanning, M., Saavedra, J., Baldo, E., 2008. New SHRIMP U—Pb data from the Famatina Complex: constraining Early—Mid Ordovician Famatinian magmatism in the Sierras Pampeanas, Argentina. Geologica Acta 6 (4), 319—333.

Davis, J.S., Roeske, S.M., McClelland, W.C., Snee, L.W., 1999. Closing the ocean between the Precordillera terrane and Chilenia: early Devonian ophiolite emplacement and deformation in the southwest Precordillera. In: Ramos, V.A., Keppie, J.D. (Eds.), Laurentia-Gondwanan connections before Pangea: Geolog-ical Society of America Special Paper 336, pp. 115—138.

Dickinson, W., Gehrels, G., 2003. U—Pb ages of detrital zircons from Permian and Jurassic eolian sandstones of the Colorado Plateau, USA: paleogeographic implications. Sedimentary Geology 163 (1—2), 29—66.

Drobe, M., López de Luchi, M., Steenken, A., Frei, R., Naumann, R., Siegesmund, S., Wemmer, C., 2009. Provenance of the late proterozoic to early cambrian metaclastic sediments of he Sierra de San Luis (Eastern Sierras Pampeanas) and Cordillera Oriental, Argentina. Journal of South American Earth 28, 239—262.

Escayola, M.P., Pimentel, M., Armstrong, R., 2007. Neoproterozoic backarc basin: sensitive high-resolution ion microprobe U—Pb and Sm—Nd isotopic evidence from the eastern Pampean Ranges, Argentina. Geology 35, 495—498.

Ezpeleta, M., Astini, R.A., Dávila, F., Cawood, P.A., 2009. SHRIMP U—Pb dating and subsidence analysis of pre-Andean Paganzo Basin, northwestern Argentina: Implications for late Paleozoic tectonic evolution of western Gondwana. Colloquium on Latin America. Abstracts and Program, 93—95. Göttingen.

Gehrels, G.E., Valencia, V.A., Ruiz, J., 2008. Enhanced precision, accuracy, efficiency, and spatial resolution of U—Pb ages by laser ablation—multicollector—inductively coupled plasma—mass spectrometry. Geochemistry, Geophysics, Geosystems 9. doi:10.1029/2007GC001805 Q03017.

Godoy, E., Wellkner, D., 2003. El Basamento de la Costa del Norte Chico, 20 años después. X Congreso Geológico Chileno. CD ROM, Concepción.

Grosse, P., Söllner, F., Báez, M., Toselli, A.J., Rossi, J.N., De la Rosa, J., 2008. Lower Carboniferous post-orogenic granites in central-eastern Sierra de Velasco, Sierras Pampeanas, Argentina: U—Pb monazite geochronology, geochemistry and Sr—Nd isotopes. International Journal of Earth Sciences 98, 1001—1025.

Gulbranson, E.L., Montañez, I.P., Schmitz, M.D., Limarino, C.O., Isbell, J.L., Marenssii, S.A., Crowley, J.L., 2010. High-precision U—Pb calibration of Carboniferous glatiation and climate history, Paganzo Group, NW Argentina. Geological Society of America Bulletin 122, 1480—1498.

Hartmann, L.A., Campal, N., Santos, J., McNaughthon, N., Bossi, J., Schiplilov, A., Lafon, J.M., 2001. Archean Crust in the Rio de la Plata Craton, Uruguay, SHRIMP U—Pb Reconaissance study. Jornal of South American Earth Sciences 14, 557—570.

Hauser, N., Matteini M., Omarini, R.H., Pimentel, M.M. Combined U—Pb and Lu—Hf isotope data on turbidites of the Paleozoic basement of NW Argentina and petrology of associated igneous rocks: Implications for the tectonic evolution of western Gondwana between 560 and 460 Ma. Gondwana Research, in press (available online).

Hongn, F.D., Tubía, J.M., Aranguren, A., Vegas, N., Mon, R., Dunning, G.R., 2010. Magmatism coeval with lower Paleozoic shelf basins in NW-Argentina (Tastil batholith): constraints on current stratigraphic and tectonic interpretations. Journal of South American Earth Sciences 29, 289—305.

Hoskin, P., Schaltegger, U., 2003. The composition of zircon and igneous and meta-morphic petrogenesis. Reviews in Mineralogy and Geochemistry 53, 27—62.

Irwin, J., García, C., Hervé, F., Brook, M., 1988. Geology of part of a long-lived dynamic plate margin: the coastal cordillera of north-central Chile, latitude 30°51′—31°S. Canadian Journal of Earth Sciences 25 (4), 603—624.

Kay, S.M., Ramos, V.A., Mpodozis, C., Sruoga, P., 1989. Late Paleozoic to Jurassic silicic magmatism at the Gondwana margin: analogy to the Middle Proterozoic in North America? Geology 17, 324—328.

Kay, S.M., Orrell, S., Abbruzzi, J.M., 1996. Zircon and whole rock Nd—Pb isotopic evidence for a Grenville age and a Laurentian origin for the Precordillera terrane in Argentina. Journal of Geology 104, 637—648.

Keppie, J.D., Ramos, V.A., 1999. Odyssey of Terranes in the Iapetus an Rheic Oceans during the Paleozoic. In: Geological Society of America, Special Paper 336 267—276.

Llambías, E.J., 1999. Las rocas ígneas Gondwánicas: 1. El magmatismo Gond-wánico durante el Paleozoico superior-Triásico. In: Caminos, R. (Ed.), Geo-logía Argentina. Servicio Geológico Minero Argentino, Buenos Aires, pp. 349—363.

Llambías, E.J., Gregori, D., Basei, M.A., Varela, R., Prozzi, C., 2003. Ignimbritas riolí-ticas neoproterozoicas en la Sierra Norte de Córdoba: ¿evidencia de un arco magmático temprano en el ciclo Pampeano? Revista de la Asociación Geológica Argentina 58 (4), 572—582.

Loewy, S., Connelly, J., Dalziel, I., 2004. An orphaned basement block: the Arequipa-Antofalla basement of the central Andean margin of south America. Geological Society of America Bulletin 116 (1—2), 171—187.

López de Azarevich, V.L., Escayola, M., Azarevich, M.B., Pimentel, M., Tassinari, C., 2009. The Guarguaraz complex and the Neoproterozoic—Cambrian evolution of southwestern Gondwana: geochemical signaturas and geochronological constraints. Journal of South American Earth Sciences 28, 333—344.

Ludwig, K.R., 2003. User's manual for Isoplot/Ex, Version 3.0, A geochronological toolkit for Microsoft Excel. Berkeley Geochronology Center, 2455 Ridge Road, Berkeley CA 94709, USA. Special Publication No. 4.

Martina, F., Viramonte, J.M., Astini, R.A., Pimentel, M.M., Dantas, E., 2007. Evidence of Early Carboniferous Pre-Choiyoi volcanism in western Gondwana: first isotopic, geochemical and U—Pb SHRIMP data. Colloquium on Latin America. Abstracts and Program, 51. Kiel.

Martina, F., Astini, R., 2009. El volcanismo "eohercínico" (Mississippiano): ¿dónde está?. In: XII Congreso Geológico Chileno, p. 4. Abstract S8-003, Santiago.

Martina, F., Viramonte, J.M., Astini, R.A., Pimentel, M.M., Dantas, E., 2010. Early-Carboniferous volcanism in the southern central Andes: new U—Pb SHRIMP zircon geochronology and whole rock geochemistry. Gondwana Research. doi:10.1016/j.gr.2010.07.004.

Massonne, H.-J., Calderón, M., 2008. P—T evolution of metapelites of the Guarguaráz complex, Argentina — evidence for Devonian crustal thickening close to the western Gondwana margin. Revista Geológica de Chile 35, 215—231.

McDonough, M.R., Ramos, V.A., Isachsen, C.E., Bowring, S.A., Vujovich, G.I., 1993. Nuevas edades de circones del basamento de la sierra de Pie de Palo, Sierras Pampeanas Occidentales de San Juan: sus implicancias para los modelos del supercontinente proterozoico de Rodinia. In: 12° Congreso Geológico Argen-tino, Actas, vol. 3, pp. 340—342. Buenos Aires.

Moscoso, R., Nasi, C., Salinas, P., 1982. Hoja Vallenar y Parte Norte de La Serena, Regiones de Atacama y Coquimbo. In: Carta Geológica de Chile, vol. 55. Servicio Nacional de Geología y Minería. Santiago100.

Mpodozis, C., Cornejo, P., 1997. El Rift Triásico-Sinemuriano de Sierra Exploradora, Cordillera de Domeyko (25—26°S) Asociaciones de facies y Reconstrucción Tec-tónica. In: Congreso Geológico Chileno N° 8, Actas, vol. 1 Antofagasta550—554.

Mpodozis, C., Ramos, V., 1989. The Andes of Chile and Argentina. In: Ericksen, G.E., Cañas, M.T., Reinemund, J.A. (Eds.), Geology of the Andes and its relation to hydrocarbon and mineral resources. Circum-Pacific Councyl for Energy and Mineral Resources Earth-Science Series, vol. 11, pp. 59—90.

Mpodozis, C., Kay, S.M., 1992. Late Paleozoic to Triassic evolution of the Gondwana margin: evidence from Chilean Frontal Cordilleran Batholiths (28°—31°S). Geological Society of America Bulletin 104, 999—1014.

Naipauer, M., Vujovich, G.I., Cingolani, C.A., McClelland, W.C., 2010. Detrital zircon análisis from the Neoproterozoic-Cambrian sedimentary cover (Cuyania terrane), Sierra de Pie de Palo, Argentina: evidence of a rift and passive margin system? Journal of South American Earth 29, 306—326.

Paces, J., Miller, J., 1993. Precise U—Pb ages of Duluth complex and related mafic intrusions, northeastern Minnesota — geochronological insights to physical, petrogenetic, paleomagnetic, and tectonomagmatic processes associated with the 1.1 Ga midcontinent rift system. Journal of Geohysical Research-Solid Earth 98 (B8), 13997—14013.

Pankhurst, R.J., Millar, I.L., Hervé, F., 1996. A Permo-Carboniferous U–Pb age for part of the Guanta unit of the Elqui–Limarí Batholith at Rio Transito, northern Chile. Revista Geológica de Chile 23, 35–42.

Ramos, V.A., 2008. The basement of the central Andes: the Arequipa and Related Terranes. Annual Review of Earth and Platetary Sciences 36, 289–324.

Ramos, V.A., 2009. Anatomy and global context of the Andes: main geologic features and the Andean orogenic cycle. In: Kay, S.M., Ramos, V.A., Dickinson, W. (Eds.), Backbone of the Americas, Shallow Subduction, Plateau Uplift and Terrane Collision. Geological Society of America, pp. 31–66. Memoir 204.

Ramos, V.A., 2010. The Grenville-age basement of the Andes. Journal of South American Earth Sciences 29, 77–91.

Ramos, V.A., Basei, M., 1997. The basement of Chilenia: an exotic continental terrane to Gondwana during the early Paleozoic. In: Terrane Dynamics 97, International Conference on Terrane Geology, pp. 140–143. Christchurch, New Zealand, Conference Abstracts.

Ramos, V.A., Jordan, T.E., Allmendinger, R.W., Kay, S.M., Cortés, J.M., Palma, M.A., 1984. Chilenia: Un terreno alóctono en la evolución paleozoica de los Andes Centrales. In: 9° Congreso Geológico Argentino, vol. 2, pp. 84–106.

Ramos, V.A., Jordan, T.E., Allmendinger, R.W., Mpodozis, C., Kay, S.M., Cortes, J., Palma, M., 1986. Paleozoic terranes of the central Argentine Chilean Andes. Tectonics 5 (6), 855–880.

Ramos, V.A., Vujovich, G., Martino, R., Otamendi, J. Pampia: a large cratonic block missing in the Rodinia supercontinent, Journal of Geodynamics, in press (available online).

Rapela, C.W., Pankhurst, R.J., Casquet, C., Baldo, E., Saavedra, J., Galindo, C., Fanning, C.M., 1998. The Pampean orogeny of the southern proto-Andes: Cambrian continental collision in the Sierras de Córdoba. In: Pankhurst, R.J., Rapela, C.W. (Eds.), The Proto-Andean Margin of Gondwana, Geological Society of London Special Publication, vol 142, pp. 181–217.

Rapela, C.W., Pankhurst, R.J., Casquet, C., Fanning, C.M., Baldo, E.G., González-Casado, J.M., Galindo, C., Dahlquist, J., 2007. El Río de la Plata craton and the assembly of SW Gondwana. Earth-Science Reviews 83, 49–82.

Rapela, C.W., Pankhurst, R.J., Casquet, C., Baldo, E., Galindo, C., Fanning, C.M., Dahlquist, J.M., 2010. The Western Sierras Pampeanas: Protracted Grenville-age history (1330–1030 Ma) of intra-oceanic arcs, subduction–accretion at continental-edge and AMCG intraplate magmatism. Journal of South American Earth Sciences 29, 105–127.

Reimann, C.R., Bahlburg, H., Kooijman, E., Berndt, J., Gerdes, A., Carlotto, V., López, C., 2010. Geodynamic evolution of the early Paleozoic Western Gondwana margin 14°–17°S reflected by the detritus of the Devonian and Ordovician basins of southern Peru and northern Bolivia, Gondwana Research, in press (available online).

Reutter, K., 1974. Entwicklung und Bauplan der chilenischen Hochkordillere im Bereich 29° südlicher Breite. Neues Jahrbuch für Geologie und Paläontologie 146 (2), 153–178.

Ribba, L., 1985. Geología regional del cuadrángulo El Tránsito, región de Atacama, Chile. Memoria para optar al título de Geólogo. Departamento de Geología, Universidad de Chile, Santiago.

Ribba, L., Mpodozis, C., Hervé, F., Nasi, C., Moscoso, R., 1988. El basamento del Valle del Tránsito, Cordillera de Vallenar: eventos magmáticos y metamórficos y su relación con la evolución de los andes chileno-argentinos. Revista Geológica de Chile 15, 126–149.

Rivano, S., Sepúlveda, P., 1991. Hoja Illapel. Región de Coquimbo. In: Carta Geológica de Chile, vol. 69. Servicio Nacional de Geología y Minería, Santiago. 132.

Salazar, E., Arriagada, C., Mpodozis, C., Martínez, F., Peña, M., Alvarez, J., 2009. Análisis Estructural del Oroclino de Vallenar: Primeros Resultados. In: 12th Congreso Geológico Chileno Abstract S9_026, Santiago.

Schwartz, J.J., Gromet, P., 2004. Provenance of a late Proterozoic–early Cambrian basin, Sierras de Córdoba, Argentina. Precambrian Research vol. 129, 1–2.

Schwartz, J.J., Gromet, P., Miró, R., 2008. Timing and duration of the Calc-Alkaline arc of the Pampean Orogeny: implications for the Late Neoproterozoic to Cambrian evolution of western Gondwana. The Journal of Geology 116, 39–61.

Siegesmund, S., Steenken, A., Martino, R.D., Wemmer, L., López de Luchi, M.G., Frei, R., Presnyakov, S., Guereschi, A., 2010. Time constraints on the tectonic evolution of the eastern Sierras Pampeanas (Central Argentina). International Journal of Earth Sciences 99, 1199–1226.

Stacey, J.S., Kramers, J.D., 1975. Approximation of terrestrial lead isotope evolution by a two-stage model. Earth and Planetary Science Letters 26 (2), 207–221.

Thomas, W.A., Astini, R.A., 2003a. The Argentine Precordillera: a traveler from the Ouachita embayment of north American Laurentia. Science 273 (5276), 752–757.

Thomas, W.A., Astini, R.A., 2003b. Ordovician accretion of the Argentine Precordillera terrane to Gondwana: a review. Journal of South American Earth Sciences 16, 67–79.

Thomas, W.A., Astini, R., Mueller, P., Gehrels, G., Wooden, J., 2004. Transfer of the Argentine Precordillera terrane from Laurentia: constraints from detrital-zircon geochronology. Geology 32 (11), 965–968.

Tohver, E., Trindade, R., Solum, J., Hall, C.M., Riccomini, C., Nogueira, A.C., 2010. Closing the Clymene ocean and bending a Brasiliano belt: evidence for the Cambrian formation of Gondwana, southeast Amazon craton. Geology 38 (3), 267–270.

Vujovich, G., van Staal, C.R., Davis, W., 2004. Age constraints on the tectonic evolution and provenance of the Pie de Palo complex, Cuyania composite terrane, and the Famatinian Orogeny in the Sierra de Pie de Palo, San Juan, Argentina. Gondwana Research 7 (4), 1041–1056.

Wasteneys, H.A., Clark, A.H., Farrar, E., Langridge, R.J., 1995. Grenvillian granulite-facies metamorphismin the Arequipa Massif, Peru: a Laurentia-Gondwana link. Earth and Planetary Science Letters 132, 63–73.

Welkner, D., Arévalo, C., Godoy, E., 2006. Geología del Area Freirina-El Morado. In: Carta geológica de Chile, Serie Geología Básica, vol. 100. Servicio Nacionalde Geología y Minería, Santiago. 50.

Willner, A.P., Thomson, S.N., Kröner, A., Wartho, J.A., Wijbrans, J., Hervé, F., 2005. Time markers for the evolution and exhumation history of a late palaeozoic paired metamorphic belt in central Chile (34°–35°30′S). Journal of Petrology 46, 1835–1858.

Willner, A.P., Gerdes, A., Massonne, H.J., 2008. History of crustal growth and recycling at the Pacific convergent margin of south America at latitudes 29°–36°S revealed by a U–Pb and Lu–Hf isotope study of detrital zircon from late paleozic accretionary systems. Chemical Geology 253, 114–129.

Willner, A.P., Massonne, H.-J., Gerdes, A., Hervé, F., Sudo, M., Thomson, S., 2009a. Does Chilenia exist? Evidence from the evolution of collisional and coastal accretionary systems between the latitudes 30°S and 35°S. Colloquium on Latin America. Abstracts and Program, 310–311.

Willner, A.P., Massonne, H.-J., Gerdes, A., Hervé, F., Sudo, M., Thomson, S., 2009b. The contrasting evolution of collisional and coastal accretionary systems between the latitudes 30°S and 35°S: evidence for the existence of a Chilenia microplate. In: 12th Congreso Geológico Chileno Abstract S9_099, Santiago.

Willner, A., Gerdes, A., Massone, H.J., Schmidt, A., Sudo, M., Thomson, S., Vujovich, G., 2011. The geodynamics of collision of a microplate (Chilenia) in Devonian times deduced by the pressure–temperature–time evolution within part of a collisional belt (Guarguaraz Complex, W-Argentina). Contributions to Mineralogy and Petrology. doi:10.1007/s00410-010-0598-8.

Wörner, G., Lezuan, J., Beck, A., Heber, V., Lucassen, R., Zinnrebe, E., Rössling, R., Wilke, H.G., 2000. Geochronology, metamorphic petrology and geochemistry of basement rocks from Belén (N. Chile) and C. Uyarani (W. Bolivian Altiplano): implications for the evolution of Andean basement. Journal of South American Earth Sciences 13, 717–737.